Journal of Medicinal Chemistry

Article

pubs.acs.org/jmc

Plakilactones from the Marine Sponge *Plakinastrella mamillaris*. Discovery of a New Class of Marine Ligands of Peroxisome Proliferator-Activated Receptor γ

Carmen Festa,[†] Gianluigi Lauro,[#] Simona De Marino,[†] Maria Valeria D'Auria,[†] Maria Chiara Monti,[#] Agostino Casapullo,[#] Claudio D'Amore,[‡] Barbara Renga,[‡] Andrea Mencarelli,[‡] Sylvain Petek,[§] Giuseppe Bifulco,[#] Stefano Fiorucci,[‡,⊥] and Angela Zampella*[,†,⊥]

[†]Dipartimento di Chimica delle Sostanze Naturali, Università di Napoli "Federico II", via D. Montesano 49, 80131 Napoli, Italy

[#]Dipartimento di Scienze Farmaceutiche e Biomediche, Università di Salerno, via Ponte don Melillo, 84084 Fisciano (SA), Italy

[‡]Dipartimento di Medicina Clinica e Sperimentale, Università di Perugia, Nuova Facoltà di Medicina e Chirurgia, Via Gerardo Dottori 1, S. Andrea delle Fratte, 06132 Perugia, Italy

[§]Institut de Recherche pour le Développement (IRD), UMR7138, CPRBI, BP529, 98713 Papeete, French Polynesia

Supporting Information

ABSTRACT: In this paper we report the isolation and the molecular characterization of a new class of PPARγ ligands from the marine environment. Biochemical characterization of a library of 13 oxygenated polyketides isolated from the marine sponge *Plakinastrella mamillaris* allowed the discovery of gracilioether B and plakilactone C as selective PPARγ ligands in transactivation assays. Both agents covalently bind to the PPARγ ligand binding domain through a Michael addition reaction involving a protein cysteine residue and the α,β-unsaturated ketone in their side chains. Additionally, gracilioether C is a noncovalent agonist for PPARγ, and methyl esters **1** and **2** are noncovalent antagonists. Structural requirements for the interaction of these agents within the PPARγ ligand binding domain were obtained by docking analysis. Gracilioether B and plakilactone C regulate the expression of PPARγ-dependent genes in the liver and inhibit the generation of inflammatory mediators by macrophages.

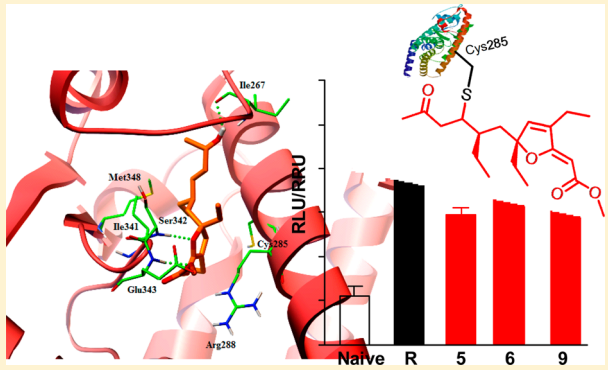

INTRODUCTION

The peroxisome proliferator-activated receptors (PPARs) are ligand-activated transcription factors belonging to the nuclear receptor superfamily. Three distinct receptor subtypes, PPARα, PPARγ, and PPARβ(δ), have been identified. While the PPAR subtypes share a high level of sequence and structural homology, each subtype has distinct physiological functions and exhibits a unique tissue expression pattern. PPARγ, the most widely investigated PPAR subtype, is predominately expressed in the adipose tissue with lower levels in heart, colon, kidney, spleen, intestine, skeletal muscle, liver, and macrophages.[1,2] PPARγ is generally recognized as a pivotal transcription factor in the regulation of adipocyte gene expression and differentiation. In addition, PPARγ has been shown to be an important regulator of target genes involved in glucose and lipid metabolism and is the mainstay of therapy for type 2 diabetes.[1,2] Furthermore, PPARγ transrepresses the expression of genes involved in inflammatory responses,[3] and suppression of the inflammatory response by PPARγ agonists is closely linked to the antidiabetic and antiatherosclerotic effects of this receptor. Thus, PPARγ agonists have been found effective in the treatment of several inflammatory and degenerative disorders including cancer, atherosclerosis, rheumatoid arthritis, and inflammatory bowel disease.

The ligand binding domain (LBD) of PPARγ allows the accommodation of a large variety of structurally different chemicals, including many food-derived substances such as polyunsaturated fatty acids, flavonoids, terpenoids, and polyphenols.[4] Despite the extraordinary chemical diversity exhibited by marine natural products, only two reports have identified marine natural products as putative PPARγ agonists. Thus, the screening of 2688 extracts from marine organisms led to the identification of psammaplin A as the first PPARγ agonist from a marine sponge.[5] Similarly, from the screening of a library of 90 bioactive marine extracts for their ability to stimulate PPARα and PPARγ transcriptional activity, sargaquinoic acid and sargahydroquinoic acid were identified as novel PPARα/γ dual agonists from *Sargassum yezoense*.[6]

Received: April 5, 2012
Published: August 30, 2012

 © 2012 American Chemical Society

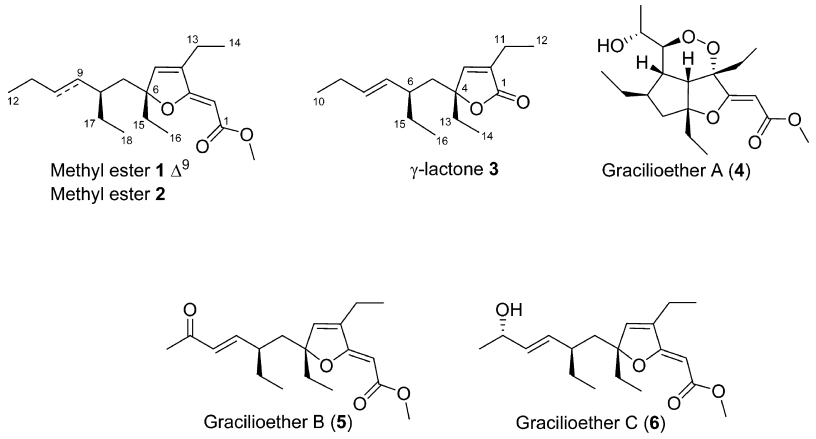

Figure 1. Known polyketides from *Plakinastrella mamillaris*.

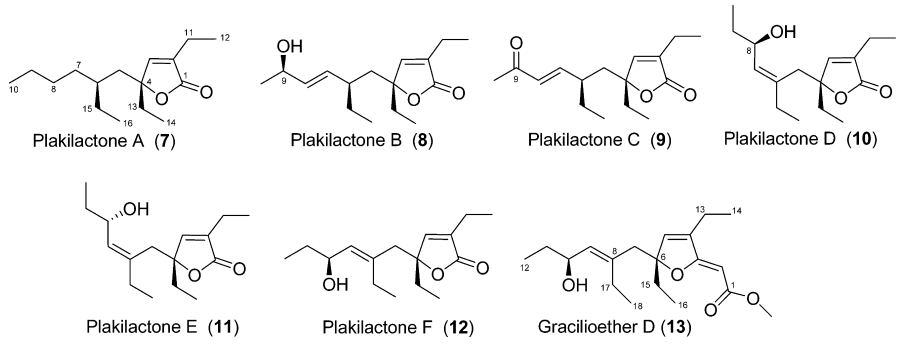

Figure 2. New compounds from *Plakinastrella mamillaris*.

As part of our search for human nuclear receptor modulators from marine organisms,[7−15] we have investigated a library of oxygenated polyketides from the sponge *Plakinastrella mamillaris*, collected at the Fiji Islands, as PPARγ modulators. Marine sponges of the genera *Plakortis* and *Plakinastrella* are known to produce a great variety of oxygenated polyketides, formed by the combination of acetyl-, propionyl-, and/or butyryl-CoA units. They include plakortolide, plakinic acid, plakortic acid, plakortone, or plakortide families.[16] Several activities have been ascribed to the members of this class, including antiproliferative,[17] antifungal, anti-inflammatory, or activation of cardiac SR-Ca^{2+}-pumping ATPase. Interestingly, compounds containing the 1,2-dioxolane system such as plakortin, plakortides, and gracilioether A exhibit potent antiprotozoan activity against *Plasmodium falciparum* and *Leishmania major*.[18−26]

In this paper we report the isolation and the molecular characterization of a library of oxygenated polyketides (Figures 1 and 2) as a new class of PPARγ ligands from the marine environment.

RESULTS

Chemistry. A specimen of *P. mamillaris* Kirkpatrick, 1900 (Homoscleromorpha) was collected at the Fiji Islands. The lyophilized sponge (171 g) was extracted with MeOH, and the combined extracts were fractionated according to the Kupchan partitioning procedure.[27]

The major components of the hexane extract were proved to be the previously reported methyl esters **1**[28] and **2**,[29] the γ-lactone **3**[28] (Figure 1), and the new γ-lactone **7** (Figure 2), which we named plakilactone A. A careful analysis of the chloroformic extract afforded several more polar derivatives such as gracilioethers A−C (**4**−**6**), previously reported from the marine sponge *Agelas gracilis* (Figure 1),[26] five new nonperoxy plakortin derivatives, plakilactones B−F (**8**−**12**), featuring the α,β-unsaturated γ-lactone moiety, and gracilioether D (**13**) showing the α,β,γ,δ-unsaturated methyl ester moiety (Figure 2).

A molecular formula of $C_{16}H_{28}O_2$, two mass units more than the parent γ-lactone **3**, was deduced for plakilactone A (**7**), $[\alpha]_D^{25}$ −9.5 (*c* 0.12, MeOH). Inspection of NMR data revealed the same cyclic core as in **3** and the saturation of the Δ^7 double bond on the side chain.

The stereochemistry at C-6 and C-8 of methyl ester (**2**) and at C-4 and C-6 of γ-lactone **3** and plakilactone A (**7**) was determined as shown in Figure 3. The 6*R*,8*R* absolute stereochemistry of methyl ester **1**, $[\alpha]_D^{25}$ −281.8 (*c* 0.40, $CHCl_3$), has been unambiguously established by chemical degradation,[30] enantioselective synthesis,[31,32] and optical rotation values.[32] As expected by chemical shift and optical rotation considerations (see Supporting Information for NMR data), when subjected to reductive ozonolysis, compounds **1** and **3** gave the same aldehyde **14**,[33] thus allowing us to establish the absolute configuration for γ-lactone **3**. Mild hydrogenation of methyl ester **1** afforded the synthetic methyl ester **2** whose NMR and optical rotation data were identical to those of the natural sample **2**.[34] Once again reductive ozonolysis of the methyl ester **2** gave a sample whose NMR and optical rotation data were identical to those of plakilactone A (**7**).[35] Therefore the absolute configuration of **7** was determined as shown in Figure 3.

dx.doi.org/10.1021/jm300911g | J. Med. Chem. 2012, 55, 8303−8317

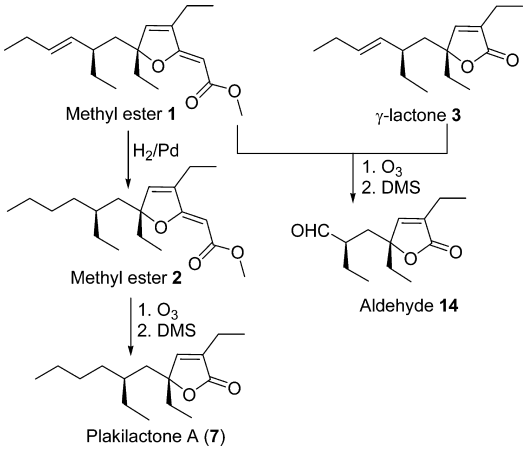

Figure 3. Stereochemical relationship between compounds **1** and **2**, **3**, **7**.

Plakilactone B (**8**), $[\alpha]_D^{25}$ −24.7 (*c* 0.05, $CHCl_3$), was analyzed for $C_{16}H_{26}O_3$ by HRESIMS. ^1H and ^{13}C NMR data (Tables 1 and 2) revealed the same nucleus as in **7**. The complete spin system of the side chain was easily inferred by COSY analysis and recognized as the same found in gracilioether C (**6**).[26] However, a careful comparison of their NMR chemical shifts evidenced small but not negligible deviations, thus suggesting an epimeric configuration at C-9. This hypothesis was confirmed by Mosher's analysis[36] that revealed an opposite 9*R* configuration of the secondary alcohol function.

Table 2. ^{13}C NMR (125 MHz, CD_3OD) Data for Plakilactones A–F (7–12) and Gracilioether D (13)

	compound						
C	7[a]	8	9	10	11	12	13
1	170.1	175.5	175.6	175.8	175.3	175.3	168.9
2	135.9	135.6	136.5	136.4	136.3	136.3	83.8
3	150.2	153.4	153.0	152.6	152.4	152.9	173.7
4	89.5	90.8	91.1	90.7	90.5	91.1	141.1
5	40.9	42.9	43.5	38.3	38.4	43.4	141.5
6	34.2	40.1	41.3	138.0	137.9	138.1	99.1
7	33.9	135.0	155.3	132.6	132.5	134.7	44.4
8	28.8	136.1	131.8	70.4	69.9	69.9	138.2
9	23.0	68.6	203.9	31.0	31.0	31.5	134.0
10	14.1	23.5	26.6	9.9	10.0	9.9	70.0
11	18.6	19.3	19.4	19.3	19.2	19.1	31.3
12	12.0	12.0	12.1	12.1	12.1	12.0	9.9
13	31.0	32.0	31.8	31.1	31.4	31.1	19.2
14	7.8	7.7	7.9	7.6	7.7	7.7	12.2
15	27.1	30.4	29.8	32.0	31.8	25.2	31.8
16	10.5	11.5	11.7	12.9	12.8	13.2	8.0
17							25.4
18							13.5
OCH_3							50.8

[a]100 MHz, $CDCl_3$.

The molecular formula $C_{16}H_{24}O_3$, assigned to plakilactone C (**9**) by HRESIMS, indicated that the compound is a dehydro derivative of **8**. Oxidation of the secondary hydroxy group at C-9 in **8** to a ketone in **9** was straightforward from the NMR data (δ_C 203.9, Table 2) and by the complete agreement of the

Table 1. ^1H NMR Data (500 MHz, CD_3OD) for Plakilactones A–F (7–12) and Gracilioether D (13)

	compound						
H	7	8	9	10	11	12	13
1	–	–	–	–	–	–	–
2	–	–	–	–	–	–	4.81 s
3	6.83 br t (1.5)	7.07 br t (1.4)	7.07 br t (1.4)	7.17 br t (1.4)	7.18 br t (1.5)	7.15 br t (1.3)	
4	–	–		–	–	–	–
5	1.58 m	1.82 ovl	1.94 dd (9.9, 14.9)	2.47 d (14.2)	2.45 d (14.3)	2.45 d (14.0)	6.50 s
	1.81 m	1.93 dd (2.3, 13.8)	2.11 ovl	2.78 d (14.2)	2.89 d (14.3)	2.58 d (14.0)	
6	1.13 ovl	1.79 ovl	2.10 ovl	–	–	–	–
7	1.13 ovl	5.29 ovl	6.62 dd (9.4, 16.0)	5.26 d (9.5)	5.28 d (9.5)	5.11 d (9.0)	2.58 d (14.4)
							2.44 d (14.4)
8	1.15 ovl	5.31 ovl	5.88 d (16.0)	4.22 dt (6.5, 9.2)	4.20 dt (6.5, 9.1)	4.18 dt (6.7, 8.8)	–
9	1.20 m	4.20 m	–	1.39 m	1.50 m	1.37 m	5.17 d (9.0)
				1.54 m		1.52 m	
10	0.89 t (6.6)	1.21 d (6.4)	2.25 s	0.90 t (7.4)	0.94 t (7.4)	0.85 t (7.5)	4.14 dt (6.6, 9.0)
11	2.32 dq (1.8, 7.5)	2.25 m	2.22 m	2.25 m	2.23 q (7.4)	2.24 q (7.5)	1.35 m
							1.48 m
12	1.18 t (7.5)	1.16 t (7.4)	1.12 t (7.4)	1.15 t (7.4)	1.13 t (7.4)	1.15 t (7.5)	0.82 t (7.4)
13	1.74 m	1.77 ovl	1.83 m	1.85 quint (7.4)	1.83 quint (7.1)	1.82 quint (7.5)	2.18 m
		1.80 ovl		1.92 quint (7.4)	1.90 quint (7.1)	1.88 quint (7.5)	
14	0.84 t (7.4)	0.78 t (7.4)	0.80 t (7.4)	0.82 t (7.4)	0.82 t (7.4)	0.81 t (7.4)	1.16 t (7.4)
15	1.30 m	1.27 m	1.38 m	1.99 q (7.6)	1.96 q (7.7)	2.03 m	1.83 quint (7.4)
		1.37 m	1.50 m			2.12 m	1.88 quint (7.4)
16	0.84 t (7.4)	0.84 t (7.5)	0.86 t (7.4)	0.98 t (7.4)	0.98 t (7.4)	0.99 t (7.5)	0.79 t (7.5)
17							1.95 m
							2.13 m
18							0.97 t (7.5)
OCH_3							3.66 s

dx.doi.org/10.1021/jm300911g | *J. Med. Chem.* 2012, 55, 8303–8317

chemical shift and coupling constant values of the side chain in **9** as compared with those of gracilioether B (**5**).[26] The close match in the chemical shift values and the negative sign of optical rotation values of plakilactones B and C and γ-lactone **3** pointed toward a 4*R*,6*R* absolute configuration in **8** and **9**.

Plakilactone D (**10**) was isolated as an optically active glassy solid, $[\alpha]_D^{25}$ −27.2 (*c* 0.05, $CHCl_3$), and had a formula of $C_{16}H_{26}O_3$ inferred from HRESIMS. ^1H and ^{13}C NMR data (Tables 1 and 2) indicated the presence of four ethyl groups, one methylene, two oxygenated carbons, two trisubstituted double bonds, and one acyl group. The same 2,4-diethyl-α,β-unsatured γ-lactone substructure as in γ-lactone **3**[28] was deduced by comparison of NMR spectroscopic data and supported by key HMBC correlations from H-3 to C-2 and C-4, from H-11 to C-1 and C-2, and from H-13 to C-4 (Figure 4).

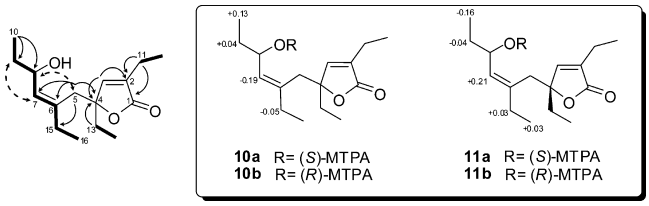

Figure 4. COSY connectivities (bold bonds), HMBC (black arrows) and ROESY (dashed arrows) correlations for plakilactones D (**10**) and E (**11**). $\Delta\delta_{S-R}$ values (ppm) of MTPA esters **10a**, **10b** and **11a**, **11b**.

An isolated AB system evidenced in the allylic region of the ^1H NMR spectrum was assigned to a methylene group and connected to C-4 and C-6 on the basis of HMBC correlations H-5a and H-5b to C-4, C-6, C-7, and C-15. The substructure C-6(C-15/C-16)/C-10 was easily deduced from COSY data (Figure 4). Therefore, the planar structure of **10** was determined as shown in Figure 4. The *Z* stereochemistry of the Δ^6 double bond was assigned on the basis of the dipolar couplings H-7/H-15, H-16 and H-5/H-8.

The absolute stereochemistry of the secondary hydroxy group at C-8 was determined by application of the modified Mosher's method.[36] Treatment of **10** with *R*-(−)- and *S*-(+)-MTPACl yielded *S*-(−)- and *R*-(+)-MTPA esters **10a** and **10b**, respectively. The $\Delta\delta$ value distribution pattern clearly indicated the 8*R* configuration (Figure 4).

Plakilactone E (**11**), $[\alpha]_D^{25}$ +8.9 (*c* 0.12, $CHCl_3$), possesses the same molecular formula ($C_{16}H_{26}O_3$ by HRESIMS) as plakilactone D (**10**) and was determined to be its C(8) epimer from the following considerations. The NMR spectroscopic data of these compounds were very similar (Tables 1 and 2), although not identical, and analysis of 2D NMR spectra of **11**, including COSY, HSQC, HMBC, and ROESY experiments, indicated the same gross structure and the same configuration of the C-6 double bond as in **10**. Mosher's analysis revealed the 8*S* configuration (Figure 4); therefore, plakilactone E (**11**) is the C-8 epimer of plakilactone D (**10**).

HRESIMS and 2D NMR data (Tables 1 and 2) indicated that plakilactone F (**12**), $[\alpha]_D^{25}$ −24.7 (*c* 0.09, $CHCl_3$), was a stereoisomer of plakilactone E (**11**). In this case, differences between the two compounds were found in the dipolar couplings inferred from the 2D ROESY spectrum, in which plakilactone F (**12**) displayed the cross-peaks H-7/H-5a, H-7/H-5b, and H-8/H-15, pointing to the *E* configuration of Δ^6 double bond.

Whereas the NMR data of **10** and **11** were almost superimposable, the configuration at the C-6 double bond had a strong influence on the chemical shifts of all nuclei of the side chain (Tables 1 and 2). Particularly diagnostic were the ^{13}C chemical shifts of C-5 and C-15, which were found downshifted (δ_C 43.4 in **12** vs 38.4 in **11**) or upshifted (δ_C 25.2 in **12** vs 31.8 in **11**), respectively, as consequence of a differentiated γ-gauche interaction with the C-8 hydroxyl group. Mosher's analysis revealed the 8*S* configuration.

Gracilioether D (**13**), $[\alpha]_D^{25}$ −11.7 (*c* 0.11, MeOH), showed the same molecular formula of gracilioether C (**6**).[26] NMR analysis (Tables 1 and 2) revealed the presence of the α,β,γ,δ-unsaturated methyl ester moiety as in **6** and a side chain identical to that of plakilactone F (**12**). The complete matching of NMR data for the side-chain nuclei with those of plakilactone F (**12**) allowed us to establish the *S* configuration at C-10 carbinol.

The 4*R* and the 6*R* configuration is proposed for plakilactones D−F (**10**−**12**) and gracilioether D (**13**), respectively, on the basis of the chemical shift values of all

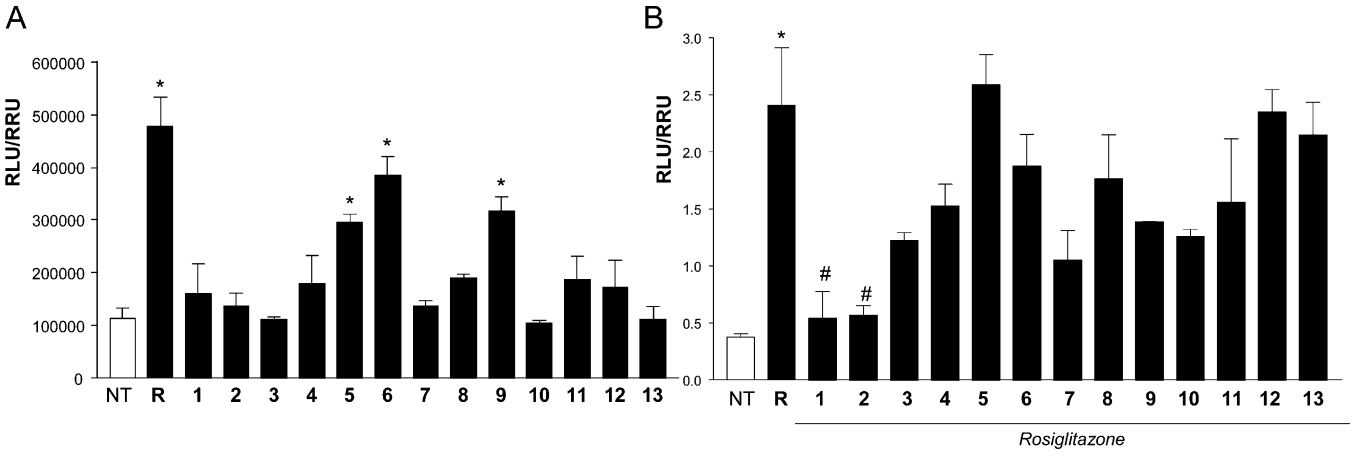

Figure 5. PPARγ transactivation assay. HepG2 cells were transiently transfected with a chimeric receptor expressing plasmid pSG5GAL4-PPARγLBD and with the reporter vector p(UAS)5_xTK-Luc. Twenty-four hour post-transfection cells were stimulated for 18 h with (A) 100 nM rosiglitazone (R) and compounds **1**−**13**, 10 μM. (B) 100 nM Rosiglitazone (R) alone or in combination with compounds **1**−**13**, 50 μM. Data are the mean ± SE of three experiments. *$P < 0.05$ versus nontreated cells (NT). #$P < 0.05$ versus rosiglitazone-stimulated cells.

dx.doi.org/10.1021/jm300911g | J. Med. Chem. 2012, 55, 8303−8317

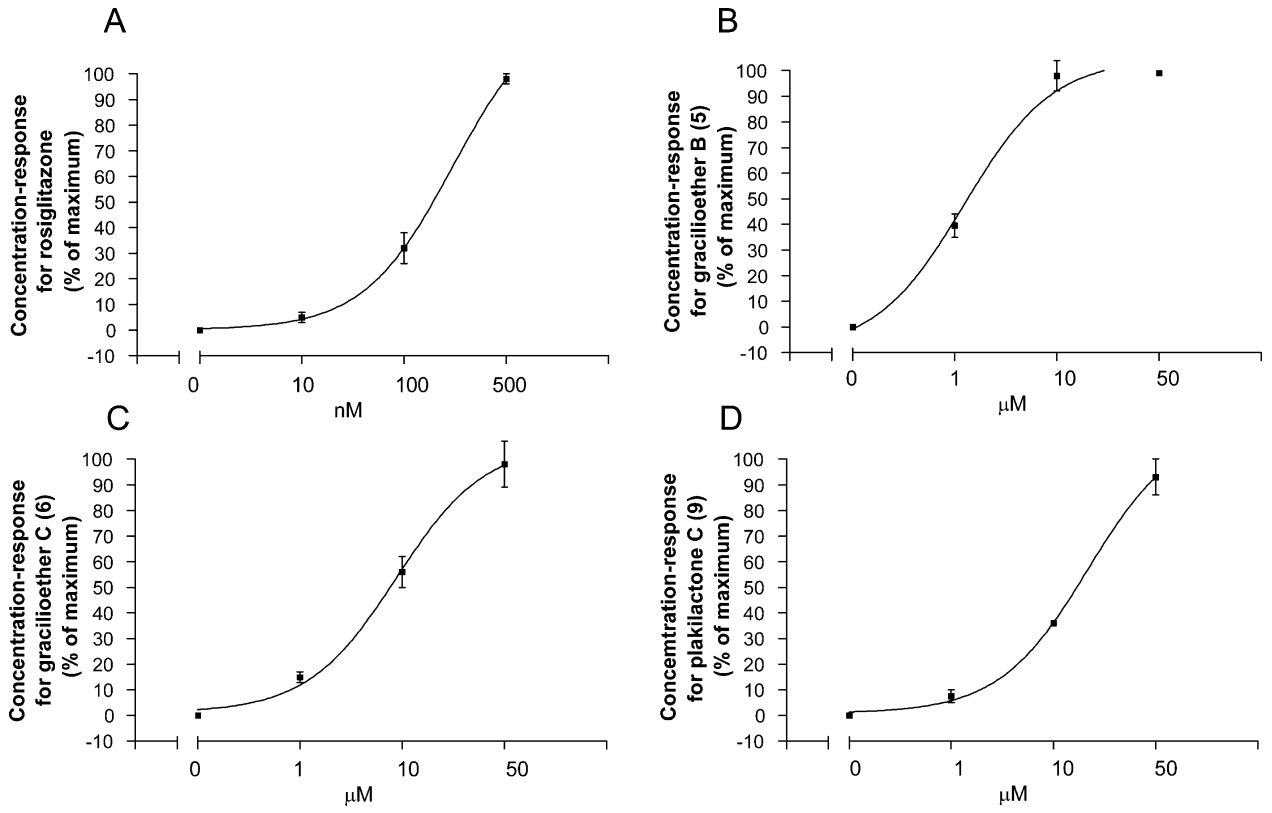

Figure 6. HepG2 cells were transiently transfected with pSG5GAL4-PPARγLBD and p(UAS)5$_x$TK-Luc. Twenty-four hour post-transfection cells were treated with increasing concentrations of (A) rosiglitazone, (B) gracilioether B (**5**), (C) gracilioether C (**6**), (D) plakilactone C (**9**), and cell extracts subsequently assayed for luciferase activity. Data are the mean ± SE of three experiments.

nuclei of the cyclic core (Tables 1 and 2), almost superimposable with those of plakilactone A (**7**) and gracilioether C (**6**).[26]

Oxygenated Polyketides from *Plakinastrella* are Selective PPARγ Ligands. PPARγ can be activated by a number of natural lipid metabolites, including oxidized fatty acids, several cyclooxygenase (COX) and lipoxygenase (LOX) metabolites, and 15-deoxy-Δ12,14-prostaglandin J2 (15d-PGJ2), the first endogenous ligand identified. These molecules act as covalent ligands possessing a common core moiety, an α,β-unsaturated ketone, able to form a covalent bond with a cysteine residue in the PPARγ–LBD through a Michael addition.[37−39]

Thus, the presence of a Michael acceptor, an α,β-unsaturated ketone, or alternatively an α,β,γ,δ-unsaturated methyl ester moiety in all polyketides isolated from *Plakinastrella* prompted us to investigate their capability to transactivate PPARγ. As shown in the Figure 5, several members of this series effectively transactivated PPARγ with compounds **5**, **6**, and **9** being the most potent agonists. In addition, when incubated in presence of the synthetic ligand rosiglitazone, methyl esters **1** and **2** attenuated the transactivation induced by this agent, thus acting as PPARγ antagonists.

To further investigate the specificity of these agents, we tested their ability to transactivate the other members of the PPAR family. As illustrated in Figures S1 and S2 in the Supporting Information, none of these agents caused a significant transactivation of PPARα and PPARβ. Thus, it appears that these agents are selective PPARγ modulators. Analysis of the concentration/response curves for transactivation of PPARγ in response to rosiglitazione and to gracilioether B (**5**), gracilioether C (**6**), and plakilactone C (**9**) demonstrates that the marine compounds activate PPARγ in a dose-dependent manner with a relative EC_{50} of ≈5, 10, and 2 μM for compounds **5**, **6**, and **9**, respectively (Figure 6).

Gracilioether B and Plakilactone C Covalently Bind to PPARγ. We then moved to a detailed analysis of the interaction mechanism at a molecular level, to assess the binding mode of these agents within PPARγ–LBD. First, a liquid chromatography-ESI MS (LC-ESI-MS)[40−42] approach was applied to detect the potential formation of PPARγ–LBD covalent complexes with gracilioether B (**5**), gracilioether C (**6**), plakilactone C (**9**), the methyl ester **1**, the γ-lactone **3**, and plakilactone B (**8**), in physiologically relevant conditions. After incubation with PPARγ–LBD, a time-course analysis of the reaction mixtures was performed for each ligand, and the chromatograms revealed the presence of stable covalent complexes solely in presence of gracilioether B (**5**) and plakilactone C (**9**). Two species were detected in the LC-MS runs of gracilioether B (**5**) and plakilactone C (**9**) (Figure 7 panel A), that were identified, on the basis of their MW, as the unmodified PPARγ–LBD (MW of 36172.7 ± 0.3 Da) and as the 1:1 PPARγ–LBD/gracilioether B (**5**) or plakilactone C (**9**) covalent adducts, the last ones giving mass increments of 320 and 264 Da, respectively, compared to the free protein (Figure 7, panel A, and Table S8 in Supporting Information). These mass differences supported the hypothesis of a Michael addition between the natural compounds and PPARγ–LBD (Figure 7 panel C).

Then we moved to the identification of the punctual site of the covalent modification on PPARγ–LBD by gracilioether B (**5**) through a combination of classical protein chemistry

dx.doi.org/10.1021/jm300911g | J. Med. Chem. 2012, 55, 8303−8317

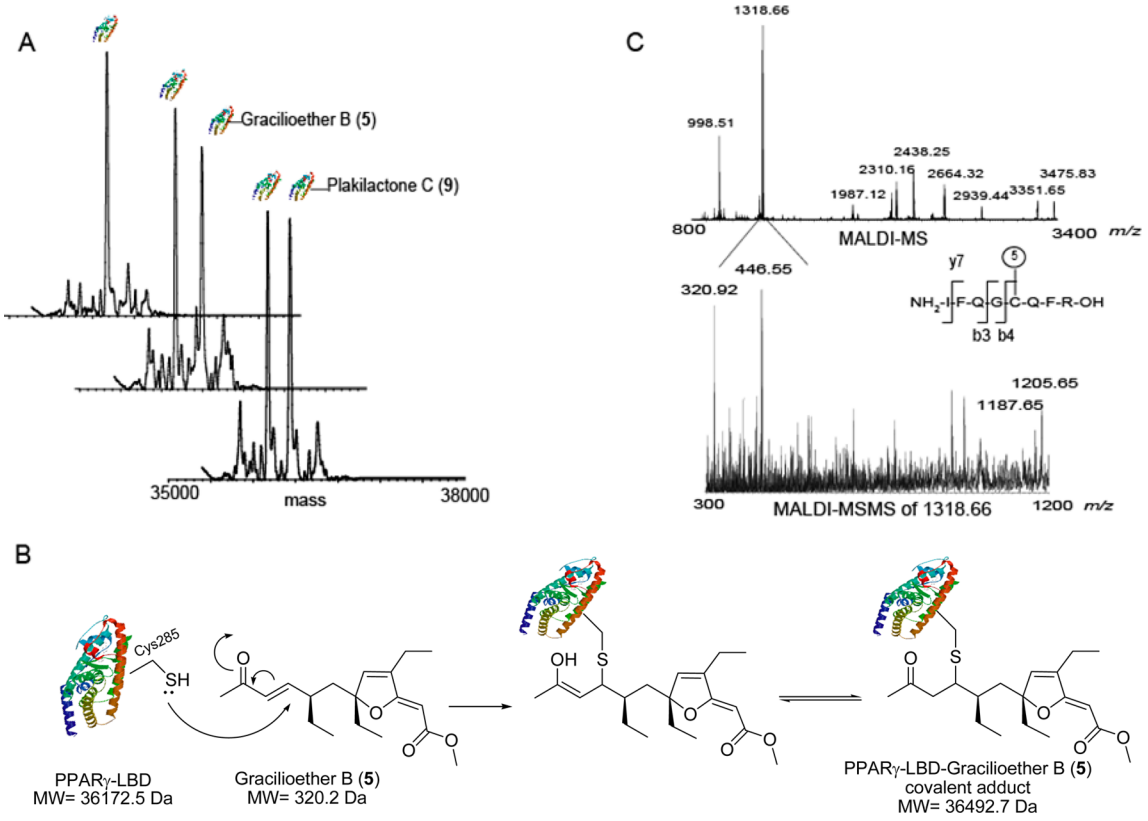

Figure 7. Panel A: deconvoluted spectra of PPARγ–LBD alone (back), upon gracilioether B (**5**) (middle) and plakilactone C (**9**) incubation (front). Panel B: mechanism of the covalent modification of PPARγ–LBD by Michael addition on the α,β-unsaturated ketone moiety in the side chain of **5** (or **9**). Panel C: MALDI-MS spectrum of PPARγ-LBD/gracilioether B (**5**) complex tryptic digestion and MALDI-MS/MS analysis of the ion at *m*/*z* 1318.66.

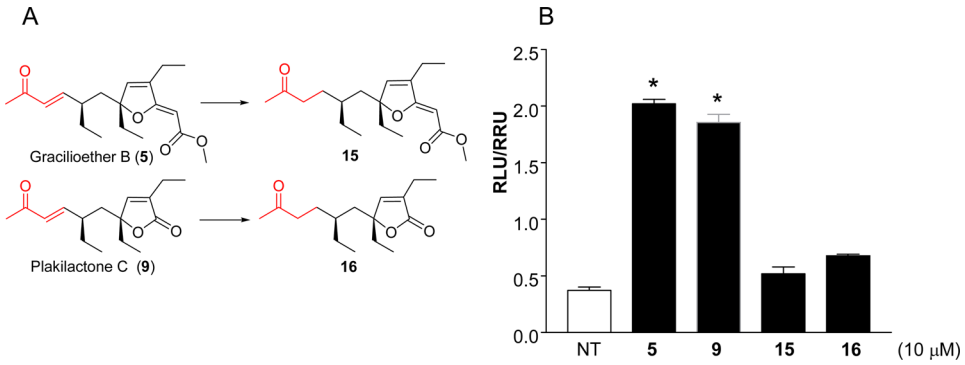

Figure 8. (A) Mild hydrogenation of gracilioether C and plakilactone C (H_2/Pt/C, 5 min, rt). (B) Luciferase reporter assay performed in HepG2 cells transiently transfected with a chimeric receptor expression plasmid pSG5GAL4-PPARγLBD and with the reporter vector p(UAS)5$_x$TK-Luc. Twenty-four hour post-transfection cells were stimulated for 18 h with 10 μM compounds **5**, **9**, **15**, and **16**. Data are the mean ± SE of three experiments. *P, 0.05 versus nontreated cells (NT).

protocols, MALDI-MS and MS/MS techniques. The chromatographic fraction containing the covalent complex was subjected to an extensive proteolysis with trypsin and analyzed by MALDI-MS. As reported in Figure 7, panel C, and Table S9 in the Supporting Information, the MALDI spectrum led us to identify a peak at *m*/*z* 1318.66, corresponding to the peptide 281–288 (NH_2-IFQGCQFR-COOH) containing the Cys285 and increased of 320.2 Da in its MW. Finally, MALDI-MS/MS analysis confirmed the correct peptide identification through the formation of the daughter ions at *m*/*z* 320.92, 446.55, and 1205.65, attributed to b3, b4, and y7 fragmentations, respectively. Thus, Cys285 was unequivocally determined as the protein residue involved in the covalent binding with gracilioether B (**5**).

On the basis of structural considerations, the α,β-unsaturated carbonyl moiety exclusively present in the side chain of gracilioether B (**5**) and plakilactone C (**9**) should act as specific Michael acceptor (Figure 7, panel B). To demonstrate this hypothesis, gracilioether B (**5**) and plakilactone C (**9**) were subjected to mild hydrogenation of the side-chain double bond, giving the derivatives **15** and **16**, respectively (Figure 8, panel A).

Derivatives **15** and **16** were separately incubated with PPARγ–LBD, subjected to LC-ESI-MS analysis (see pre-

dx.doi.org/10.1021/jm300911g | J. Med. Chem. 2012, 55, 8303–8317

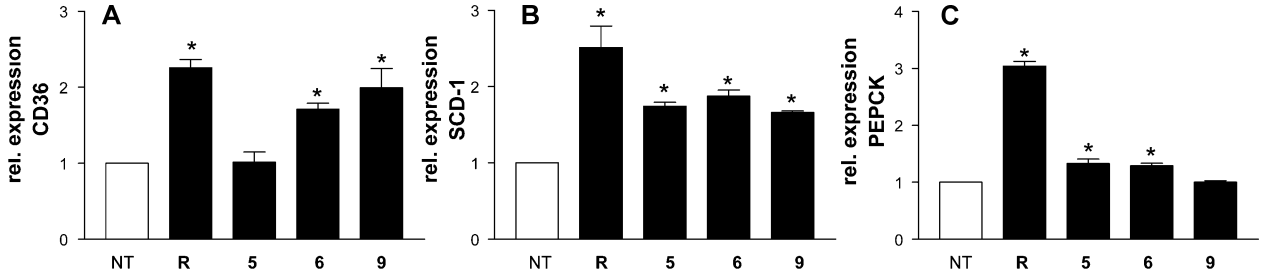

Figure 9. Serum-starved HepG2 cells were stimulated for 18 h with 100 nM of rosiglitazone (R) or gracilioethers B (**5**) and C (**6**) and plakilactone C (**9**), 10 μM. Total RNA was extracted to perform real-time PCR of (A) CD36, (B) SCD-1, and (C) PEPCK. Values were normalized relatively to GAPDH mRNA and are expressed relatively to content of these genes in untreated cells, which are arbitrarily set to 1. Analysis was carried out in triplicate, and the experiment was repeated twice. *P < 0.05 versus nontreated cells.

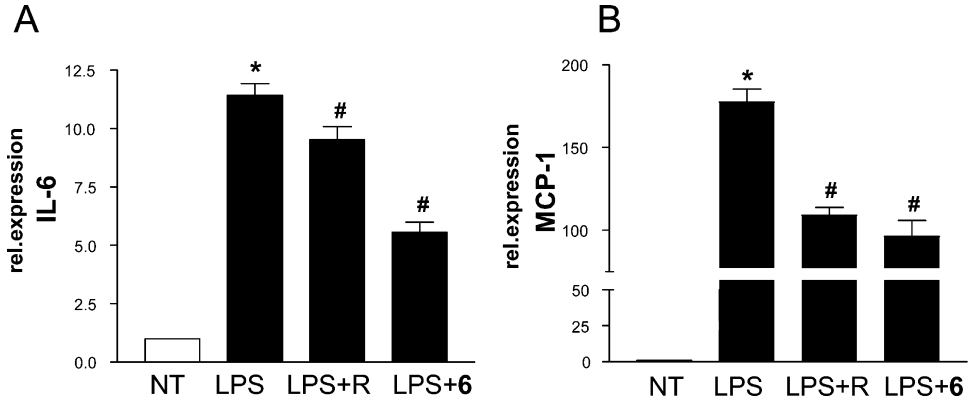

Figure 10. Serum-starved THP-1 cells were pretreated for 3 h with 100 nM rosiglitazone (R) or gracilioether C (**6**), 10 μM, before the administration of LPS (1 μg/mL) for 18 h. Total RNA was extracted to analyze the relative mRNA expression of (A) IL-6 and (B) MCP-1 by real-time PCR. Values were normalized with respect to GAPDH mRNA and are expressed with respect to those of the untreated cells, which were arbitrarily set to 1. The analysis was carried out in triplicate, and the experiment was repeated twice. *P < 0.05 versus nontreated cells. #P < 0.05 versus LPS-treated cells.

viously) and, as expected, were unable to form covalent adducts with the PPARγ–LBD (Table S8 in the Supporting Information) and, importantly, to transactivate PPARγ (Figure 8, panel B). All these data unequivocally revealed that the Cys285 targets the α,β-unsaturated carbonyl moiety on the side chain of gracilioether B (**5**) and plakilactone C (**9**), moreover confirming graciliother C (**6**) and methyl esters **1** and **2** as noncovalent PPARγ ligands.

Gene Expression Regulation by Gracilioethers B and C and Plakilactone C. We next examined whether gracilioethers B (**5**) and C (**6**) and plakilactone C (**9**) regulate the expression of genes that are known targets of PPARγ in HepG2, a human hepatocarcinoma cell line, and in THP-1, a human monocytic leukemia cell line. For this purpose, HepG2 cells were exposed to rosiglitazone or gracilioethers B (**5**) and C (**6**) and plakilactone C (**9**), and the relative mRNA expression of SCD-1 (stearoyl-CoA desaturase-1), CD36 (cluster of differentiation 36), and PEPCK (phosphoenolpyruvate carboxykinase)[43,44] were assessed by quantitative RT-PCR. As shown in Figure 9, gracilioether B (**5**), gracilioether C (**6**), and plakilactone C (**9**) exhibited a pattern of pharmacological activities full compatible with their ability to bind and transactivate PPARγ. All these agents increased the expression of SCD-1. Furthermore, gracilioether C (**6**) and plakilactone C (**9**) increased the expression of CD36, and gracilioethers B (**5**) and C (**6**) the expression of PEPCK.

Finally, we measured whether glacilioether C (**6**), the noncovalent PPARγ agonist, effectively modulated PPAR-regulated genes in macrophages, a prototypical target of this nuclear receptor. As shown in Figure 10, pretreating of THP-1 cells with rosiglitazone or gracilioether C (**6**) counter-regulated the induction of both the pro-inflammatory cytokine IL-6 (interleukine-6) and the MCP-1 (monocyte chemotactic protein-1) chemokine caused by LPS administration.

Docking Studies. To rationalize the binding mode in PPARγ of the aforementioned compounds, docking calculations and molecular dynamics simulations were performed using Autodock-Vina[45] and Macromodel 8.5 software packages, respectively, taking into account that gracilioether B (**5**) and plakilactone C (**9**) are covalent ligands. In this context, it should be mentioned that the activation of PPARγ by a covalent ligand depends also on its ability to establish, apart from the covalent bond, additional weak interactions in the LBD.[37,38,46]

Indeed, Waku et al.[39] proposed a model, defined "dock and lock", in which the first step (docking step) involves several noncovalent interactions of the putative ligand in the LBD, whereas in the second step (locking step) the covalent binding to the Cys285 is observed. As the apo and the locked form of this protein showed remarkable structural differences, in our docking studies on the covalent ligands **5** and **9**, two crystallographic structures of PPARγ were used: the apo-form (PDB code: 2ZK0) and a covalent complexed form with nitro-233 (PDB code: 2ZK5),[39] that was removed before the docking of our compounds. The docking poses of gracilioether B (**5**), gracilioether C (**6**), and plakilactone C (**9**), the most active

dx.doi.org/10.1021/jm300911g | J. Med. Chem. 2012, 55, 8303–8317

components of the library, were compared with the antagonists, methyl esters **1** and **2**, and with the inactive compounds plakilactone B (**8**) and gracilioether D (**13**). Within this approach, we confirmed that the active covalent ligands are docked in the apo form in poses compatible with the positioning of their reactive moieties around the Cys285, showing at the same time several interactions with key amino acid residues in the LBD. In the locked form of the receptor, we first tried to analyze the formation of the covalent bond using the recently introduced covalent docking methodologies.[47] Unfortunately, using the flexible side-chain method, a restricted space in the binding site of PPARγ was observed, thus determining steric clashes after the formation of the covalent bond. On the other hand, using the covalent grid-based approach, poses compatible with the covalent bond were found but with unfavorable predicted binding energies. For these reasons, we concluded that putative models of the covalent ligands could be better detected by using molecular dynamics simulations, analyzing their motions in the LBD of PPARγ. Results from these experiments allowed us to identify some significant poses in which the distances between the reactive part of these molecules and the sulfur atom on the Cys285 were compatible with the formation of the C−S covalent bond.

Noncovalent Ligands. The docking model in the apo form shows that the noncovalent agonist gracilioether C (**6**) entails a set of weak interactions, with the OH group in the side chain determining a favorable accommodation in the LBD of PPARγ. In particular, in the apo form, **6** establishes van der Waals interactions with the Ile341 and the Met348, and polar interactions with the Arg288. Three hydrogen bonds stabilize the compound in the LBD, between the ether oxygen of the cycle and the NH of the Ser342, between the terminal oxygen of the ester moiety and the NH of the Glu343, and finally between the OH at position-11 and the CO group of the Ile267 (Figure 11).

Methyl esters **1** and **2** differ from gracilioether C (**6**) for the presence of a fully hydrophobic side chain that causes a different orientation in the PPARγ−LBD, with a flip of the ring of ∼180° on the major axis of the compounds (Figure 12a) and then with the loss of some essential interactions. Indeed, we found alternative poses in which the $\alpha,\beta,\gamma,\delta$-unsaturated methyl ester moiety of **6**, **1**, and **2** are well superimposed (Figure 12b), but also in this case the hydrophobic side chains of **1** and **2** do not allow any polar interaction as observed for **6**, mainly the hydrogen bond with the Ile267. As demonstrated for 15d-PGJ$_2$, this residue plays a fundamental role in the activity of a putative PPARγ covalent agonist. Indeed, even if the covalent binding at the Cys285 is maintained, mutations at this residue abolish the transcriptional activation induced by this endogenous PPARγ agonist.[39]

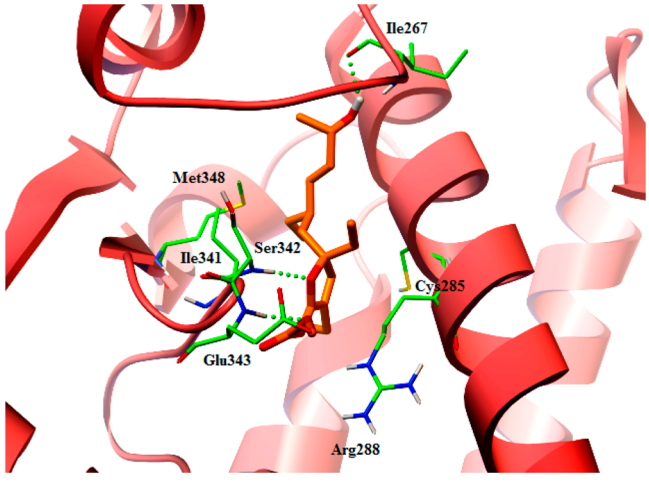

Figure 11. Gracilioether C (**6**) (colored by atom types: C orange, O red, OH hydrogen light gray) in docking with PPARγ−LBD of the apo form. Residues are colored by atom type: C green, H light gray, O red, N blue, S yellow.

Similar considerations could be also applied for gracilioether D (**13**). In this case, the superposition with the gracilioether C (**6**) shows a similar orientation of the $\alpha,\beta,\gamma,\delta$-unsaturated methyl ester core but a different accommodation of the side chain with the OH group at C-10 far from the Ile267 (Figure 12c). In summary, the inverted configuration at C-10 and the presence of a Δ^8 double bond with respect to the side chain of gracilioether C (**6**) could explain the loss of the bioactivity for **13**.

Of interest is the case of the inactive plakilactone B (**8**) displaying the same lactone moiety of plakilactone C (**9**) and the side chain of gracilioether C (**6**). Its accommodation in the PPARγ−LBD is inverted (Figure 12d), probably due to the absence of the $\alpha,\beta,\gamma,\delta$-unsaturated methyl ester moiety. As a consequence, the smaller cyclic α,β-unsaturated lactone moiety is oriented to form a hydrogen bond with the Ile267, and the OH in the side chain is able to establish only one hydrogen bond (Leu340) where **6** generated a wide set of polar interactions. In summary, **8** shows some potential interesting points in its chemical structure, but in perfect agreement with absence of activity toward PPARγ, the inability to create a covalent bond and the presence of a small cyclic part cause an unstable placement in the LBD.

Covalent Agonists. For gracilioether B (**5**) a docking pose in the apo form of PPARγ in which the α,β-unsaturated ketone in the side chain is oriented toward the Cys285 was found, and this conformation is stabilized by several hydrogen bonds between the $\alpha,\beta,\gamma,\delta$-unsaturated methyl ester moiety and the Cys285, showing a strong point of attachment of the compound in proximity of this residue. Moreover, **5** establishes further polar interactions with the Ile281 and the Arg288, as well as hydrophobic interactions with Met264, Leu330, and Ile341 (Figure 13a). Therefore, as previously demonstrated,[39] in the "docking step" a putative covalent ligand searches, through a wide range of weak interactions, the best conformation favorable to the covalent bond.

In the locked form, a conformation in which the α,β-unsaturated ketone of **5** is close to the Cys285 (distance between the sulfur of Cys285 and the reactive β-carbon of the α,β-unsaturated ketone of **5** = 3.439 Å) was found. Starting from this conformation, several fast steps of molecular dynamics simulations were applied, observing a gradual reduction of this distance.

When a pose with a distance between these groups compatible with the C−S covalent bond was found (∼1.8 Å), the covalent bond was manually generated and the complex was processed to a further fast step of molecular dynamics simulation (Figure 13b). As previously reported, several alterations in the regions following the helix H2′ and a considerable rearrangement of the helices H3 and H12 could be observed, comparing the apo form and the locked form of the receptor (Figure 13c).[39]

Similarly, the side-chain α,β-unsaturated ketone of plakilactone C (**9**) is prone to function as a Michael acceptor and, in

dx.doi.org/10.1021/jm300911g | J. Med. Chem. 2012, 55, 8303−8317

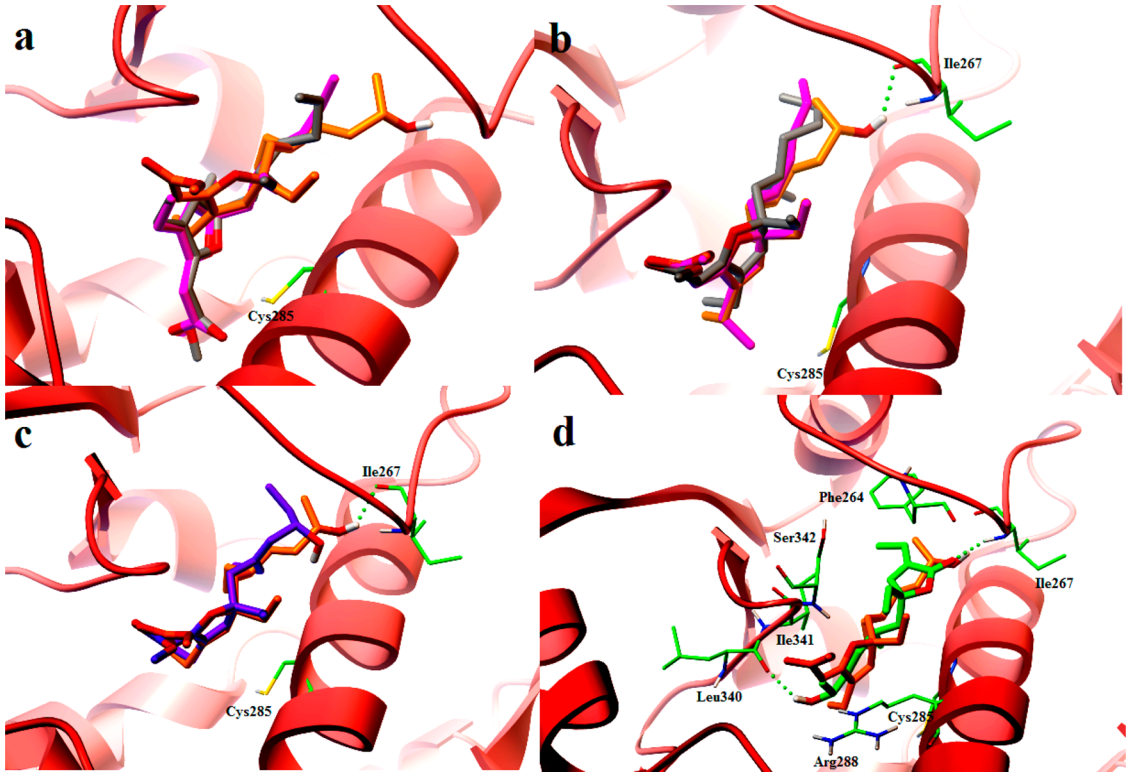

Figure 12. Superimposition between **6** (colored by atom types: C orange, O red, OH hydrogen light gray) and (a) first docking model and (b) alternative docking model of **1** (colored by atom types: C gray, O red) and **2** (colored by atom types: C purple, O red); (c) gracilioether D (**13**) (colored by atom types: C violet, O red, OH hydrogen light gray); (d) plakilactone B (**8**) (colored by atom types: C green, O red, OH hydrogen light gray) in docking with PPARγ–LBD of the apo form. Residues are colored by atom type: C green, H light gray, O red, N blue, S yellow. Hydrogen bonds are displayed with green spheres.

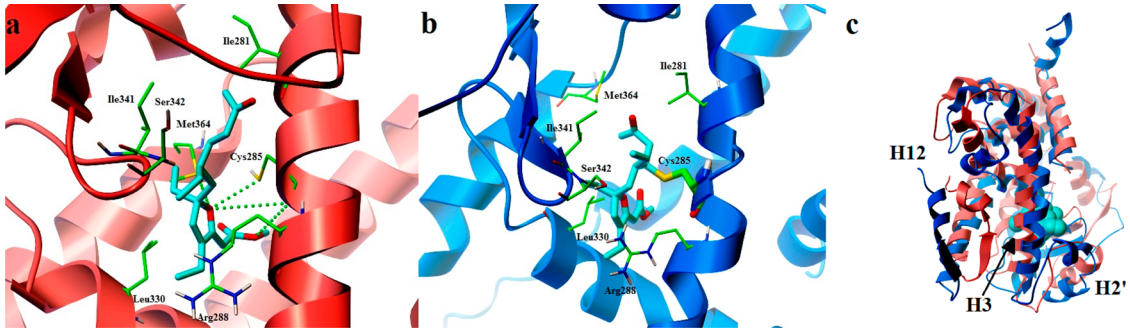

Figure 13. Docking and covalent models of gracilioether B (**5**) (colored by atom types: C sky blue, O red) in docking with PPARγ–LBD of (a) the apo form and (b) the locked form after molecular dynamics simulations. Residues are colored by atom type: C green, H light gray, O red, N blue, S yellow. (c) Superimposition between the apo form of PPARγ (secondary structure represented in red) and the locked form complexed with gracilioether B (**5**) (secondary structure represented in blue; **5** is in CPK representation and colored by atom types: C sky blue, O red).

Figure 14a, a pose in the apo form in which this moiety is near to Cys285 is shown. A hydrogen bond was observed between the carbonyl oxygen of the α,β-unsaturated lactone moiety and the NH of Ile267 (Figure 14a)[39] as well as further polar interactions are established between the cyclic core and Arg288 and His266.

In the locked form of PPARγ, the docking results confirmed the nearness of the α,β-unsaturated ketone in the side chain of **9** to Cys285 (distance between the sulfur of Cys285 and the reactive β-carbon of the α,β-unsaturated ketone of **9** = 3.918 Å). As for **5**, this complex (Figure 14b) was processed through molecular dynamics simulations, observing also in this case the rearrangement of the helices H3, H12, and H2′ (Figure 14c).

DISCUSSION AND CONCLUSION

In the present study we report the isolation and pharmacological characterization of a family of oxygenated polyketides from the *Plakinastrella mamillaris* sponge. The detailed analysis of pharmacological properties of these agents allowed us to demonstrate that members of this library are robust and selective ligands of the nuclear receptor PPARγ. PPARγ is a well validated pharmacological target. Thiazolidinedione, rosiglitazone, and pioglitazone are potent PPARγ agonists and insulin-sensitizers and have been extensively used in the treatment of type 2 diabetes. Thiazolidinediones induce the transcription of PPARγ responsive genes and control lipid synthesis and storage in adipose tissue, the liver, and many

dx.doi.org/10.1021/jm300911g | J. Med. Chem. 2012, 55, 8303–8317

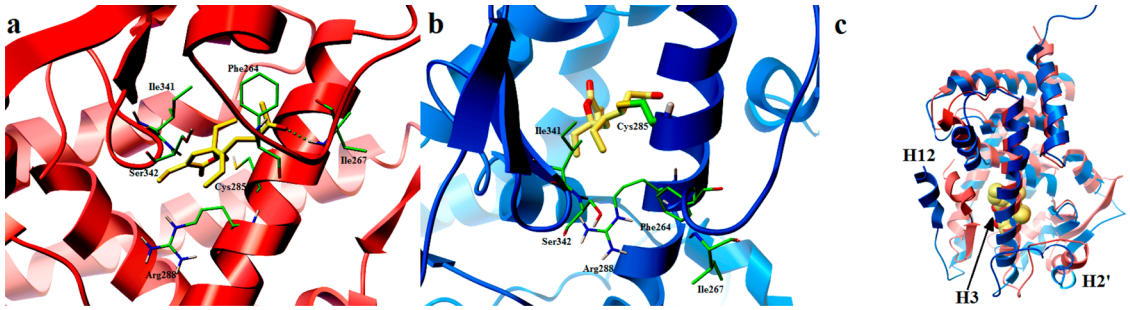

Figure 14. Docking and covalent models of plakilactone C (**9**) (colored by atom types: C light yellow, O red) in docking with PPARγ–LBD of (a) the apo form and (b) the locked form after molecular dynamics simulations. Residues are colored by atom type: C green, H light gray, O red, N blue, S yellow. Hydrogen bonds are displayed with green spheres. (c) Superimposition between the apo form of PPARγ (secondary structure represented in red) and the locked form complexed with plakilactone C (**9**) (secondary structure represented in blue; **9** is in CPK representation and colored by atom types: C light yellow, O red).

other tissues; however, their use is associated with side effects including weight gain, fluid retention, and increased risk of heart failure. Rosiglitazone was withdrawn from the market in 2011, and pioglitazone is contraindicated in patients with New York Heart Association (NYHA) Class III or IV heart failure in the USA, while in Europe is contraindicated in patients with any stage of heart failure.[44,48−53] Despite the fact that pioglitazone does not increase the risk of myocardial infarction and its use is associated with a reduction in all-cause mortality, there is an urgent need for development of novel PPARγ agonists or modulators.

Previous studies from our group have led to the demonstration that marine organisms are a rich source of ligands for nuclear receptors. Thus, we have identified ligands for two major targets, the farnesoid-X-receptor (FXR) and the pregnane-X-receptor (PXR).[4] Furthermore, the marine environment, mainly sponge organisms, has been reported as the source of nuclear receptor antagonists,[12,54] which are currently being developed for their biomedical potential.

Members of this oxygenated polyketides library showed the ability to activate PPARγ in a transactivation assay in HepG2 cells transfected with a viral vector containing the LBD of the receptor whereas others reversed the effect of the synthetic ligand rosiglitazone, thus acting as PPARγ antagonists. Results from these studies demonstrated that gracilioether B (**5**), gracilioether C (**6**), and plakilactone C (**9**) activate the receptor with an EC_{50} ranging from 2 to 9 μM and are therefore 20−90 fold less potent than rosiglitazone whose EC_{50} is ≈100 nM in this assay. Despite their reduced potency, the efficacy of gracilioether B (**5**), gracilioether C (**6**), and plakilactone C (**9**) in term of receptor transactivation was very similar to that of rosiglitazone (≈80%), and in addition, all three compounds effectively triggered the transcription of PPARγ-regulated genes, although with a difference in the relative potency (Figure 9). Using HepG2 cells, we have shown that gracilioether C (**6**) and plakilactone (**9**) induce the expression of CD36, a scavenger receptor involved in the hepatic uptake of oxidized lipoprotein, a typical effect of PPARγ ligands in the liver. Interestingly, gracilioether B (**5**) fails to increase the expression of this gene in HepG2. This finding might be of relevance because increased expression of CD36 caused by PPARγ ligands is thought to mediate lipid accumulation in macrophages and the liver. Thus, the fact that gracilioether B (**5**) causes a different pattern of gene expression in comparison to rosiglitazone, might be associated with a specific pharmacological profile in vivo. In addition, we also demonstrated that gracilioether B (**5**), gracilioether C (**6**), and plakilactone C (**9**) increase the expression of SCD-1 in liver cells. SCD-1 catalyzes the rate-limiting reaction of monounsaturated fatty acid synthesis and plays an important role in the development of a fatty liver. Finally, we demonstrated that gracilioether B (**5**) and gracilioether C (**6**) but not plakilactone C (**9**) up-regulate the expression of PEPCK. PEPCK is a rate-limiting enzyme involved in gluconeogenesis and glyceroneogenesis pathways, and its expression is tightly regulated at the transcriptional level by hormones controlling glucose homeostasis with glucagon and glucocorticoids having a strong gluconeogenic action while insulin inhibits hepatic gluconeogenesis by repressing the expression of this gene.[55] The expression of PEPCK is positively regulated by different transcription factors and coactivators including hepatic nuclear factor 4α (HNF4α), Forkhead box O1 (Foxo1), and PPARγ, while the PPARγ coactivator 1 alpha (PGC1-α) has been shown to cooperate in regulating the expression of this gene in the fasting state. Induction of PEPCK in HepG2 cells by rosiglitazone and gracilioethers B (**5**) and C (**6**) is therefore of interest. Indeed, because HepG2 cells are grown in a low glucose medium, induction of PEPCK expression drives cell metabolism to glycerogenesis rather that gluconeogenesis and might be involved in development of lipid accumulation in hepatocytes, a common side effect in the rosiglitazone therapy.[55] All together these data suggest the possibility to develop novel PPARγ modulators.

Because gracilioether C (**6**) activates PPARγ in a non-covalent fashion, we have then investigated whether this agent still exerts the same range of effects as that of rosiglitazone. Using THP-1, a monocytic cell line, we demonstrated that gracilioether C (**6**) effectively modulates the expression of two inflammatory mediators, IL-6 and MCP-1. Thus, similarly to rosiglitazone, gracilioether C (**6**) causes a robust attenuation of the expression of IL-6 and MCP-1 triggered by LPS. Because the inhibition of proinflammatory mediators is a common theme in the pharmacology of PPARγ ligands, present data provide a robust evidence that gracilioether C (**6**) might be a potential agent in the treatment of inflammatory disorders.[56,57]

At molecular level we demonstrated that gracilioether B (**5**) and plakilactone C (**9**) covalently bind to a cysteine residue in the PPARγ–LBD through a Michael addition reaction to the α,β-unsaturated ketone in their side chains. Such findings were also supported by an integrated analysis of docking and molecular dynamics simulations. Besides the fact that Cys285 is

dx.doi.org/10.1021/jm300911g | J. Med. Chem. 2012, 55, 8303−8317

conserved in all three PPAR subtypes, gracilioether B (**5**) and plakilactone C (**9**) showed a significant specificity toward PPARγ. This finding indicates, as previously reported for several selective covalent PPARγ ligands,[58,59] that other amino acid residues confer specificity in the recognition process to PPARγ–LBD and moreover points toward the importance of the docking step in which the putative covalent ligand establishes several noncovalent interactions.

Also for gracilioether C (**6**), a detailed docking analysis was performed to rationalize the structural requirements for its noncovalent interaction in the receptor's LBD, and insights were gained to explain its peculiar mode of action. The analysis of the docking poses in comparison with the antagonists methyl esters **1** and **2** and several nonactive members of this series clarified the chemical requirements for the PPARγ agonistic activity and could be useful for the future de novo design and for the prediction of the bioactivity of a set of new ligands.

Also the discovery that methyl esters **1** and **2** are PPARγ antagonists[60] that counteract the receptor transactivation caused by rosiglitazone is noteworthy. Because PPARγ antagonists are of pharmacological and therapeutic relevance, we are currently elaborating on these structures to gain further insights on their pharmacological profiles.

In conclusion, this study discloses a new class of marine PPARγ ligands structurally unrelated to all synthetic and natural ligands so far reported and reaffirms the extraordinary chemodiversity and therapeutic potential of marine natural compounds.

EXPERIMENTAL SECTION

General Procedures. Specific rotations were measured on a Perkin-Elmer 243 B polarimeter. All ESI-MS spectra and LC-ESI-MS analyses were performed on a Waters Q-ToF Premiere spectrometer equipped with a Waters 2695 HPLC System and ESI source and LTQ XL ThermoScientific. MALDI spectra were recorded on a MALDI micro-MX (Waters, Co., Milford, MA). NMR spectra were obtained on Varian Inova 500 NMR spectrometer (^{1}H at 500 MHz, ^{13}C at 125 MHz, respectively) and Varian Inova 400 MHz spectrometer (^{13}C NMR at 100 MHz) equipped with Sun hardware, δ (ppm), J in hertz, spectra referred to CD_3OD (δ_H 3.31, δ_C 49.0) and $CDCl_3$ (δ_H 7.27, δ_C 77.0) as internal standards. HPLC was performed using a Waters Model 510 pump equipped with a Waters Rheodine injector and a differential refractometer, model 401. Through-space ^{1}H connectivities were evidenced using a ROESY experiment with mixing times of 200 and 500 ms, respectively. Silica gel (200–400 mesh) from Macherey-Nagel Company was used for flash chromatography. The purities of compounds were determined to be greater than 95% by HPLC.

Sponge Material and Separation of Individual Compounds. *Plakinastrella mamillaris* Kirkpatrick, 1900 (order Homosclerophorida, family Plakinidae) was collected at the Fiji Islands, in May 2007. The samples were frozen and lyophilized to yield 171 g of dry mass. The sponge was identified by Dr. John Hooper, Queensland Museum, Brisbane, Australia, where a voucher specimen is deposited under the accessing number G322695. The lyophilized material (171 g) was extracted with methanol (3 × 1.5 L) at room temperature, and the crude methanol extract (40 g) was subjected to a modified Kupchan's partitioning procedure. The methanol extract was dissolved in a mixture of MeOH/H_2O containing 10% H_2O and partitioned against *n*-hexane to give 17.3 g of the crude extract. The water content (% v/v) of the MeOH extract was adjusted to 30% and partitioned against $CHCl_3$ to give 16.6 g of the crude extract. The aqueous phase was concentrated to remove MeOH and then extracted with *n*-BuOH (2.4 g of crude extract).

The $CHCl_3$ extract (1.0 g) was chromatographed by silica gel MPLC using a solvent gradient system from CH_2Cl_2 to CH_2Cl_2:MeOH 1:1. Fractions eluted with CH_2Cl_2:MeOH 99:1 (604 mg) were further purified by HPLC on a Nucleodur 100-5 C18 (5 μm; 10 mm i.d. × 250 mm) with 70% MeOH:H_2O as eluent (flow rate 3.5 mL/min) to give 0.7 mg of plakilactone C (**9**) (t_R = 22.5 min), 2.5 mg of plakilactone F (**12**) (t_R = 23.5 min), 2.8 mg of plakilactone E (**11**) (t_R = 28.0 min), 2.6 mg of plakilactone D (**10**) (t_R = 31.0 min), 2.9 mg of plakilactone B (**8**) (t_R = 34.5 min), 5.0 mg of gracilioether A (**4**) (t_R = 36.5 min), 8.0 mg of gracilioether B (**5**) (t_R = 45.0 min), 1.9 mg of gracilioether D (**13**) (t_R = 59.0 min), and 4.2 mg of gracilioether C (**6**) (t_R = 70.0 min).

The *n*-hexane extract (8 g) was fractionated by silica gel MPLC using a solvent gradient system from *n*-hexane to EtOAc. The fraction eluted with hexane:EtOAc 98:2 (995 mg) was further purified by HPLC on a Nucleodur 100-5 C18 (5 μm; 10 mm i.d. × 250 mm) with 90% MeOH:H_2O as eluent (flow rate 5 mL/min) to give 12.5 mg of γ-lactone **3** (t_R = 5.4 min), 2.5 mg of plakilactone A (**7**) (t_R = 6.4 min), 3.5 mg of methyl ester **2** (t_R = 8.6 min). The fraction eluted with hexane:EtOAc 96:4 (2.35 g) was purified on a Nucleodur 100-5 C18 (5 μm; 10 mm i.d. × 250 mm) with 90% MeOH:H_2O as eluent (flow rate 3.5 mL/min) to give 1.9 g of methyl ester **1** (t_R = 10.8 min).

Characteristic Data for Each Compounds. *Methyl Ester **1**.* pale yellow oil; $[\alpha]_D^{25}$ −281.8 (*c* 0.40, $CHCl_3$); ^{1}H NMR data in CD_3OD given in Supporting Information; ESI-MS: *m*/*z* 329.2 $[M + Na]^+$.

*Methyl ester **2**.* pale yellow oil; $[\alpha]_D^{25}$ −69.2 (*c* 0.20, $CHCl_3$); ^{1}H NMR data in CD_3OD given in Supporting Information; ESI-MS: *m*/*z* 331.2 $[M + Na]^+$.

*γ-Lactone **3**.* pale yellow oil; $[\alpha]_D^{25}$ −11.4 (*c* 0.10, MeOH); ^{1}H NMR data in CD_3OD given in Supporting Information; ESI-MS: *m*/*z* 273.2 $[M + Na]^+$.

*Gracilioether A (**4**).* colorless solid; $[\alpha]_D^{25}$ +7.5 (*c* 0.19, MeOH).

*Gracilioether B (**5**).* colorless solid; $[\alpha]_D^{25}$ −77.2 (*c* 0.08, $CHCl_3$).

*Gracilioether C (**6**).* colorless solid; $[\alpha]_D^{25}$ −54.5 (*c* 0.12, $CHCl_3$).

*Plakilactone A (**7**).* pale yellow oil; $[\alpha]_D^{25}$ −9.5 (*c* 0.12, MeOH); ^{1}H CD_3OD and ^{13}C NMR data in $CDCl_3$ given in Tables 1 and 2; ESI-MS: *m*/*z* 275.2 $[M + Na]^+$. HRMS (ESI): calcd for $C_{16}H_{28}NaO_2$: 275.1987; found 275.1980 $[M + Na]^+$.

*Plakilactone B (**8**).* colorless solid; $[\alpha]_D^{25}$ −24.7 (*c* 0.05, $CHCl_3$); ^{1}H and ^{13}C NMR data in CD_3OD given in Tables 1 and 2; ESI-MS: *m*/*z* 289.2 $[M + Na]^+$. HRMS (ESI): calcd for $C_{16}H_{26}NaO_3$: 289.1780; found 289.1768 $[M + Na]^+$.

*Plakilactone C (**9**).* colorless solid; $[\alpha]_D^{25}$ −63.7 (*c* 0.11, $CHCl_3$); ^{1}H and ^{13}C NMR data in CD_3OD given in Tables 1 and 2; ESI-MS: *m*/*z* 287.2 $[M + Na]^+$. HRMS (ESI): calcd for $C_{16}H_{24}NaO_3$: 287.1623; found 287.1615 $[M + Na]^+$.

*Plakilactone D (**10**).* colorless solid; $[\alpha]_D^{25}$ −27.2 (*c* 0.05, $CHCl_3$); ^{1}H and ^{13}C NMR data in CD_3OD given in Tables 1 and 2; ESI-MS: *m*/*z* 289.2 $[M + Na]^+$. HRMS (ESI): calcd for $C_{16}H_{26}NaO_3$: 289.1780; found 289. 1778 $[M + Na]^+$.

*Plakilactone E (**11**).* colorless solid; $[\alpha]_D^{25}$ +8.9 (*c* 0.12, $CHCl_3$); ^{1}H and ^{13}C NMR data in CD_3OD given in Tables 1 and 2; ESI-MS: *m*/*z* 289.2 $[M + Na]^+$. HRMS (ESI): calcd for $C_{16}H_{26}NaO_3$: 289.1780; found 289.1775 $[M + Na]^+$.

*Plakilactone F (**12**).* colorless solid; $[\alpha]_D^{25}$ −24.7 (*c* 0.09, $CHCl_3$); ^{1}H and ^{13}C NMR data in CD_3OD given in Tables 1 and 2; ESI-MS: *m*/*z* 289.2 $[M + Na]^+$. HRMS (ESI): calcd for $C_{16}H_{26}NaO_3$: 289.1780; found 289.1769 $[M + Na]^+$.

*Gracilioether D (**13**).* colorless solid; $[\alpha]_D^{25}$ −11.7 (*c* 0.11, MeOH); ^{1}H and ^{13}C NMR data in CD_3OD given in Tables 1 and 2; ESI-MS: *m*/*z* 345.2 $[M + Na]^+$. HRMS (ESI): calcd for $C_{19}H_{30}NaO_4$: 345.2042; found 345.2036 $[M + Na]^+$.

Preparation of MTPA Esters 8a,b, 10a,b, 11a,b, 12a,b. A 0.5–1.0 mg sample was dissolved in freshly distilled CH_2Cl_2 and treated with triethylamine (10 μL), (−)- or (+)-α-methoxy-α-(trifluoromethyl)phenylacetyl chloride (MTPA-Cl) (5 μL), and a catalytic amount of 4-(dimethylamino)pyridine. The mixture was left to stand at room temperature for 12 h, with the resulting mixture purified by silica gel column.

*[(S)-MTPA ester of **8a**].* selected ^{1}H NMR (500 MHz, CD_3OD) δ (ppm): 7.00 (s, H-3), 5.53 (m, H-9), 5.39 (dd, J = 8.5, 15.4 Hz, H-8),

dx.doi.org/10.1021/jm300911g | J. Med. Chem. 2012, 55, 8303–8317

5.23 (dd, J = 6.8, 15.4 Hz, H-7), 1.40 (d, J = 6.5 Hz, H_3-10), 1.13 (t, J = 7.5 Hz, H_3-12).

*[(R)-MTPA ester of **8b**]*. selected ^{1}H NMR (500 MHz, CD_3OD) δ (ppm): 7.00 (s, H-3), 5.53 (m, H-9), 5.53 (dd, J = 8.8, 15.4, H-8), 5.36 (dd, J = 7.2, 15.4 Hz, H-7), 1.33 (d, J = 6.5 Hz, H_3-10), 1.12 (t, J = 7.5 Hz, H_3-12).

*[(S)-MTPA ester of **10a**]*. selected ^{1}H NMR (500 MHz, CD_3OD) δ (ppm): 7.22 (br t, J = 1.4 Hz, H-3), 5.53 (m, H-8), 5.18 (d, J = 9.8 Hz, H-7), 2.63−2.96 (d, J = 14.4 Hz, H_2-5), 2.26 (m, H_2-11), 2.07 (m, H_2-15), 1.88 (m, H_2-13), 1.63−1.69 (m, H_2-9), 1.16 (t, J = 7.4 Hz, H_3-12), 0.99 (t, J = 7.4 Hz, H_3-10), 0.97 (t, J = 7.4 Hz, H_3-16), 0.80 (t, J = 7.4 Hz, H_3-14).

*[(R)-MTPA ester of **10b**]*. selected ^{1}H NMR (500 MHz, CD_3OD) δ (ppm): 7.21 (br t, J = 1.4 Hz, H-3), 5.59 (m, H-8), 5.37 (d, J = 9.9 Hz, H-7), 2.65−2.94 (d, J = 14.3 Hz, H_2-5), 2.25 (m, H_2-11), 2.12 (m, H_2-15), 1.88 (m, H_2-13), 1.35−1.65 (m, H_2-9), 1.17 (t, J = 7.4 Hz, H_3-12), 1.01 (t, J = 7.4 Hz, H_3-16), 0.86 (t, J = 7.4 Hz, H_3-10), 0.79 (t, J = 7.4 Hz, H_3-14).

*[(S)-MTPA ester of **11a**]*. selected ^{1}H NMR (500 MHz, CD_3OD) δ (ppm): 7.22 (br t, J = 1.3 Hz, H-3), 5.62 (m, H-8), 5.33 (d, J = 10.1 Hz, H-7), 2.41−3.38 (d, J = 14.4 Hz, H_2-5), 2.22 (m, H_2-11), 1.96 (m, H_2-15), 1.92 (m, H_2-13), 1.70 (m, H_2-9), 1.11 (t, J = 7.4 Hz, H_3-12), 0.97 (t, J = 7.3 Hz, H_3-16), 0.87 (t, J = 7.4 Hz, H_3-14), 0.85 (t, J = 7.3 Hz, H_3-10).

*[(R)-MTPA ester of **11b**]*. selected ^{1}H NMR (500 MHz, CD_3OD) δ (ppm): 7.22 (br t, J = 1.3 Hz, H-3), 5.55 (m, H-8), 5.13 (d, J = 10.0 Hz, H-7), 2.42−3.40 (d, J = 14.2 Hz, H_2-5), 2.22 (m, H_2-11), 1.94 (m, H_2-13), 1.93 (m, H_2-15), 1.74 (m, H_2-9), 1.13 (t, J = 7.4 Hz, H_3-12), 1.01 (t, J = 7.3 Hz, H_3-10), 0.94 (t, J = 7.3 Hz, H_3-16), 0.89 (t, J = 7.4 Hz, H_3-14).

*[(S)-MTPA ester of **12a**]*. selected ^{1}H NMR (500 MHz, CD_3OD) δ (ppm): 7.12 (br t, J = 1.3 Hz, H-3), 5.59 (m, H-8), 5.22 (d, J = 10.1 Hz, H-7), 2.48−2.60 (d, J = 14.4 Hz, H_2-5), 2.25 (m, H_2-11), 2.23 (m, H_2-15), 1.81 (m, H_2-13), 1.51−1.63 (m, H_2-9), 1.14 (t, J = 7.4 Hz, H_3-12), 1.01 (t, J = 7.3 Hz, H_3-16), 0.79 (t, J = 7.3 Hz, H_3-10), 0.77 (t, J = 7.4 Hz, H_3-14).

*[(R)-MTPA ester of **12b**]*. selected ^{1}H NMR (500 MHz, CD_3OD) δ (ppm): 7.10 (br t, J = 1.4 Hz, H-3), 5.60 (m, H-8), 5.08 (d, J = 9.9 Hz, H-7), 2.43−2.58 (d, J = 14.4 Hz, H_2-5), 2.30 (m, H_2-11), 2.21 (m, H_2-15), 1.79 (m, H_2-13), 1.60−1.73-(m, H_2-9), 1.12 (t, J = 7.5 Hz, H_3-12), 1.02 (t, J = 7.5 Hz, H_3-16), 0.90 (t, J = 7.5 Hz, H_3-10), 0.75 (t, J = 7.4 Hz, H_3-14).

Preparation of Compound 15. An oven-dried 10 mL flask was charged with 10% platinum on carbon (2 mg) and gracilioether B (**5**) (1.7 mg, 0.0053 mmol). Absolute methanol (1 mL) and dry THF (1 mL) were added, and the flask was evacuated and flushed with argon and then with hydrogen. The reaction was stirred at room temperature under H_2 (1 atm) for 5 min. The mixture was filtered through Celite, and the recovered filtrate was concentrated. The residue was purified by HPLC on a Nucleodur 100-3 C18 (3 μm; 4.6 mm i.d. × 250 mm) with 75% MeOH:H_2O as eluent (flow rate 1 mL/min) to give 1.3 mg of **15** (t_R 20.4 min).

*Compound **15**.* colorless solid; $[\alpha]_D^{22}$ −15.2 (c 0.04, MeOH); ESI-MS: m/z 345.2042 $[M + Na]^+$. HRMS (ESI): calcd for $C_{19}H_{30}NaO_4$:345.2042; found 345.2034 $[M + Na]^+$.

Preparation of Compound 16. Plakilactone C (**9**) (2.6 mg, 0.0098 mmol) was subjected to hydrogenation as described for compound **15**. The residue was purified by HPLC on a Nucleodur 100-3 C18 (3 μm; 4.6 mm i.d. × 250 mm) with 75% MeOH:H_2O as eluent (flow rate 1 mL/min) to give 2.3 mg of compound **16** (t_R 15.0 min).

*Compound **16**.* colorless solid; $[\alpha]_D^{25}$ −19.8 (c 0.07, MeOH); ESI-MS: m/z 289.2 $[M + Na]^+$. HRMS (ESI): calcd for $C_{16}H_{26}NaO_3$:289.1780; found 289.1775 $[M + Na]^+$.

Cell Culture. HepG2 cells were maintained at 37 °C in E-MEM containing 10% fetal bovine serum (FBS), 1% L-glutamine, and 1% penicillin/streptomycin. Serum-starved HepG2 cells were stimulated for 18 h with 100 nM of rosiglitazone, 10 μM gracilioethers B (**5**) and C (**6**) or plakilactone C (**9**), and relative mRNA levels of PEPCK, SCD-1, and CD36 were analyzed by real-time PCR.

THP-1 cells were maintained at 37 °C in RPM-I containing 10% FBS, 1% L-glutamine, and 1% penicillin/streptomycin. Serum-starved THP-1 cells were pretreated with 100 nM of rosiglitazone or glacilioether C (**9**) for 3 h before the addition of 1 μg/mL LPS. After 18 h stimulation, total RNA was extracted to assess the relative mRNA levels of IL-6 and MCP-1 by real-time PCR.

Luciferase Assay. HepG2 cells were transiently transfected with the reporter vector $p(UAS)_{5X}$TK-Luc, with pGL4.70hRluc as internal control to normalize relative luciferase units, and with a vector containing the ligand binding domain of PPARγ fused with the DBD of GAL4 (pSG5GAL4PPARγLBD). Forty eight hours post-transfection, cells were stimulated for 18 h with 100 nM rosiglitazone and 10 μM compounds **1**−**13**, or with the combination of 100 nM rosiglitazone and 50 μM compounds **1**−**13**. In another experimental setting, cells were treated with increasing concentrations of **5** (1, 10, and 50 μM), **6** (1, 10, and 50 μM), **9** (1, 10, and 50 μM), or rosiglitazone (10, 100, and 500 nM).

To investigate the PPARα-mediated transactivation, HepG2 cells were transiently transfected with the reporter vector $p(UAS)_{5X}$TK-Luc, with pRFN26REN as internal control to normalize relative luciferase units, and with a vector containing the ligand binding domain of PPARα fused with the DBD of GAL4 (pSG5GAL4PPARαLBD). Forty eight hours post-transfection, cells were stimulated for 18 h with 10 μM of gemfibrozil or compounds **1**−**13**.

To investigate the PPARβ-mediated transactivation, HepG2 cells were transiently transfected with the reporter vector $p(UAS)_{5X}$TK-Luc, with pRFN26REN as internal control to normalize relative luciferase units, and with a vector containing the ligand binding domain of PPARβ fused with the DBD of GAL4 (pSG5GAL4PPARβLBD). Forty eight hours post-transfection, cells were stimulated for 18 h with 10 μM of arachidonic acid or compounds **1**−**13**.

Real-Time PCR. Total RNA was extracted using TRIzol reagent (Invitrogen), purified from the genomic DNA by DNAase I treatment (Invitrogen) and random reverse-transcribed with Superscript II (Invitrogen). A 50 ng template was amplified using the following reagents: 0.2 μM of each primer and 12.5 μL of 2X SYBR Green qPCR master mix (Invitrogen). All reactions were performed in triplicate, and the thermal cycling conditions were as follows: 2 min at 95 °C, followed by 40 cycles of 95 °C for 20 s, 55 °C for 20 s, and 72 °C for 30 s in an iCycler iQ instrument (Biorad). The relative mRNA expression was calculated and expressed as $2^{-(\Delta\Delta Ct)}$. Primers used for qRT-PCR were as follows. hGAPDH: GAAGGTGAAGGTCGGAGT and CATGGGTGGAATCATATTGGAA; hPEPCK: TCCTGGAAGAATAAGGAGTGGA and ATAATGCCTTCAATGGGAACAC; hSCD-1: GCAGAATGGAGGAGATAAGT and AATCAAAGTGATCCCATACA; hCD36: TTTCTGTATGCAAGTCCTGAT and ATTAAGCCAAAGAATAGGCAC; hIL-6: AGGAGACTTGCCTGGTGAAA and CAGGGGTGGTTATTGCATCT; hMCP-1: CCCCAGTCACCTGCTGTTAT and TCCTGAACCCACTTCTGCTT.

Analysis of PPARγ−LBD/Agonist Covalent Complex by MS. PPARγ−LBD was purchased from Bertin-Pharma. It consists of the region 195−477 of PPARγ with a hexahistidine tag at N-terminal and an unknown 24 amino acid linker region between the His tag and the sequence. For peptide identification, we used the sequence and numeration of the entire PPARγ.

PPARγ−LBD (1 μM) was separately incubated with methyl ester **1**, γ-lactone **3**, gracilioether B (**5**), gracilioether C (**6**), plakilactone B (**8**), plakilactone C (**9**), **15**, and **16** (each at 20 μM) in PBS buffer at pH 7.5 and 37 °C for 60 and 180 min. Aliquots of the mixtures were analyzed by RP-LC-MS, loading the sample on a Jupiter C4 column (50 mm × 2 mm) at 0.15 mL/min and eluting by means of a linear gradient from 20% to 70% aqueous acetonitrile containing TFA (0.05%) and formic acid (1%) over 25 min. Mass spectra were collected in an m/z range of 1500−3000.

Identification of PPARγ−LBD Modification Site by MALDI-MS and MALDI-MSMS. Twenty microliters of PPARγ−LBD/gracilioether B (**5**) complex were subjected to extensive proteolysis by trypsin using a E:S ratio of 1:100 for 1 h at 37 °C. The mixture was loaded on a C18 ZIP-TIP and eluted as reported by manufactures.

One microliter of eluted sample was analyzed by MALDI-MS in reflectron positive ion mode by using α-cyano-4-hydroxycinnamic acid (10 mg/mL) dissolved in H_2O/CH_3CN (50:50, v/v) TFA (0.1%) as matrix, in a m/z range of 700−5000. The same spot was analyzed using the MALDI source on a Q-ToF Premier spectrometer. The signal at m/z 1308.66 was selected and fragmented using MALDI laser energy of 380.0, a trigger threshold of 700, a signal threshold of 80, V_{eff} of 5523.00, MALDI extraction of 10.0, ion energy of 1.0, and collision energy of 25.0.

Computational Details. *Chemical Structures Preparation.* The chemical structures of the compounds were built and processed with Macromodel 8.5 (Schrödinger, LLC, New York, 2003). Molecular mechanics/dynamics calculations were performed on a 4 × AMD Opteron SixCore 2.4 GHz using Macromodel 8.5 and the OPLS force field. The Monte Carlo multiple minimum (MCMM) method (5000 steps) was used to allow a full exploration of the conformational space. Molecular dynamics simulations were performed at 600 K and with a simulation time of 10 ns. A constant dielectric term, mimicking the presence of the solvent, was used to reduce artifacts. Finally, the optimization (conjugate gradient, 0.05 Å convergence threshold) of the structures was applied to identify the three-dimensional starting models for the subsequent steps of docking calculations.

Docking Calculations. Docking calculations were performed using the Autodock-Vina software. In the configuration files of the two crystallographic structures of PPARγ we specified only the exhaustiveness value to 64 and the coordinate values for the targets, focusing the grid on the site of presumable pharmacological interest. In particular a grid box size of 22 × 22 × 30 and centered at 17.464 (x), 64.919 (y), and 19.625 (z) was used for the PPARγ receptor (apo form), and of 20 × 20 × 20 and centered at 17.654 (x), 64.696 (y), and 11.136 (z) (locked form), with spacing of 1.0 Å between the grid points. For all the investigated compounds, all open-chain bonds were treated as active torsional bonds. Docking results were analyzed with Autodock Tools 1.4.5.

Molecular Dynamics Simulations. Molecular dynamics simulations steps were performed for the compounds **5** and **9** to observe their contacts with the reactive counterpart of PPARγ, using Macromodel 8.5. In each step, the distances between the sulfur of Cys285 and the reactive β-carbon of the α,β-unsaturated ketone parts of **5** and **9** were constrained to reduce the distance at 0.5 Å. The obtained structures were reprocessed until a distance and an orientation of the reactive moieties compatible with the C−S bond were found. In all these steps, for the equilibration phase, an equilibration time of 10 ps was considered. Molecular dynamics simulations were performed at 300 K, with a time step of 4.0 fs and a simulation time of 0.1 ns. Then the covalent bond between the reactive points was manually built, and the two covalent complexes (**5** or **9** with PPARγ) were subjected to a further fast molecular dynamics simulation to eliminate eventual steric clashes. In all the simulations, a constant dielectric term, mimicking the presence of the solvent, was used in to reduce artifacts. Illustrations of the 3D models were generated using the Python software.[61]

■ ASSOCIATED CONTENT

Ⓢ Supporting Information

Tabulated NMR data for compounds **1**−**13**, mass details on covalent complexes, and PPARα and PPARβ transactivations. This material is available free of charge via the Internet at http://pubs.acs.org.

■ AUTHOR INFORMATION

Corresponding Author

*Tel: (0039) 081-678525. Fax (0039) 081-678552. E-mail: angela.zampella@unina.it..

Author Contributions

⊥Contributed equally to this work.

Notes

The authors declare no competing financial interest.

■ ACKNOWLEDGMENTS

We thank the Fiji government for giving us the authorization to collect and work on Fijian sponges, the fisheries department and Klaus Feussner (USP) for their help. This work was supported by grants from the Coral Reef Initiative in the South Pacific (CRISP), MIUR (PRIN 2009) "Sostanze ad attività antitumorale: isolamento da fonti marine, sintesi di analoghi e ulteriore sviluppo della chemoteca ″LIBIOMOL" and "Design, conformational and configurational analysis of novel molecular platforms" and the University of Salerno (FARB ex 60%). NMR spectra were provided by the CSIAS, Centro Interdipartimentale di Analisi Strumentale, Faculty of Pharmacy, University of Naples.

■ ABBREVIATIONS USED

CD36, cluster of differentiation 36; COX, cyclooxygenase; 15d-PGJ2, 15-deoxy-Δ12,14-prostaglandin J2; FBS, fetal bovine serum; HDAC, histone deacetylase; HepG2, human hepatoma cell line; IL-6, interleukine-6; LBD, ligand binding domain; LOX, lipoxygenase; LPS, lipopolysaccharide; MCP-1, monocyte chemotactic protein-1; MTPA-Cl, α-methoxy-α-(trifluoromethyl)phenylacetyl chloride; PDB, protein data bank; PEPCK, phosphoenolpyruvate carboxykinase; PPAR, peroxisome proliferator-activated receptor; R, rosiglitazone; ROESY, rotating frame nuclear Overhauser effect spectroscopy; RT-PCR, real time polymerase chain reaction; SCD-1, stearoyl-CoA desaturase-1; THP-1, human monocytic leukemia cell line

■ REFERENCES

(1) Heikkinen, S.; Auwerx, J.; Argmann, C. A. PPARgamma in human and mouse physiology. *Biochim. Biophys. Acta* **2007**, *1771*, 999−1013.

(2) Tontonoz, P.; Spiegelman, B. M. Fat and beyond: the diverse biology of PPARgamma. *Annu. Rev. Biochem.* **2008**, *77*, 289−312.

(3) Pascual, G.; Fong, A. L.; Ogawa, S.; Gamliel, A.; Li, A. C.; Perissi, V.; Rose, D. W.; Willson, T. M; Rosenfeld, M. G.; Glass, C. K. A SUMOylation-dependent pathway mediates transrepression of inflammatory response genes by PPAR-gamma. *Nature* **2005**, *437*, 759−763.

(4) D'Auria, M. V.; Sepe, V.; Zampella, A. Natural ligands for nuclear receptors: biology and potential therapeutic applications. *Curr. Top. Med. Chem.* **2012**, *12*, 637−669.

(5) Mora, F. D.; Jones, D. K.; Desai, P. V.; Patny, A.; Avery, M. A.; Feller, D. R.; Smillie, T.; Zhou, Y. D.; Nagle, D. G. Bioassay for the identification of natural product-based activators of peroxisome proliferator-activated receptor-gamma (PPARgamma): the marine sponge metabolite psammaplin A activates PPARgamma and induces apoptosis in human breast tumor cells. *J. Nat. Prod.* **2006**, *69*, 547−552.

(6) Kim, S. N.; Choi, H. Y.; Lee, W.; Park, G. M.; Shin, W. S.; Kim, Y. K. Sargaquinoic acid and sargahydroquinoic acid from *Sargassum yezoense* stimulate adipocyte differentiation through PPARalpha/gamma activation in 3T3-L1 cells. *FEBS Lett.* **2008**, *582*, 3465−3472.

(7) Sepe, V.; Bifulco, G.; Renga, B.; D'Amore, C.; Fiorucci, S.; Zampella, A. Discovery of sulfated sterols from marine invertebrates as a new class of marine natural antagonists of farnesoid-X-receptor. *J. Med. Chem.* **2011**, *54*, 1314−1320.

(8) Festa, C.; De Marino, S.; D'Auria, M. V.; Bifulco, G.; Renga, B.; Fiorucci, S.; Petek, S.; Zampella, A. Solomonsterols A and B from *Theonella swinhoei*. The first example of C-24 and C-23 sulfated sterols from a marine source endowed with a PXR agonistic activity. *J. Med. Chem.* **2011**, *54*, 401−405.

(9) Sepe, V.; Ummarino, R.; D'Auria, M. V.; Mencarelli, A.; D'Amore, C.; Renga, B.; Zampella, A.; Fiorucci, S. Total synthesis and pharmacological characterization of solomonsterol A, a potent marine pregnane-X-receptor agonist endowed with anti-inflammatory activity. *J. Med. Chem.* **2011**, *54*, 4590−4599.

(10) De Marino, S.; Ummarino, R.; D'Auria, M. V.; Chini, M. G.; Bifulco, G.; Renga, B.; D'Amore, C.; Fiorucci, S.; Debitus, C.; Zampella, A. Theonellasterols and conicasterols from *Theonella swinhoei*. Novel marine natural ligands for human nuclear receptors. *J. Med. Chem.* **2011**, *54*, 3065−3075.
(11) De Marino, S.; Sepe, V.; D'Auria, M. V.; Bifulco, G.; Renga, B.; Petek, S.; Fiorucci, S.; Zampella, A. Towards new ligands of nuclear receptors. Discovery of malaitasterol A, a unique bis-secosterol from marine sponge *Theonella swinhoei*. *Org. Biomol. Chem.* **2011**, *9*, 4856−4862.
(12) Renga, B.; Mencarelli, A.; D'Amore, C.; Cipriani, S.; D'Auria, M. V.; Sepe, V.; Chini, M. G.; Monti, M. C.; Bifulco, G.; Zampella, A.; Fiorucci, S. Discovery that theonellasterol a marine sponge sterol is a highly selective FXR antagonist that protects against liver injury in cholestasis. *PLoS One* **2012**, *7*, e30443.
(13) De Marino, S.; Ummarino, R.; D'Auria, M. V.; Chini, M. G.; Bifulco, G.; D'Amore, C.; Renga, B.; Mencarelli, A.; Petek, S.; Fiorucci, S; Zampella, A. 4-Methylenesterols from *Theonella swinhoei* sponge are natural pregnane-X-receptor agonists and farnesoid-X-receptor antagonists that modulate innate immunity. *Steroids* **2012**, *77*, 484−495.
(14) Chini, M. G.; Jones, C. R.; Zampella, A.; D'Auria, M. V.; Renga, B.; Fiorucci, S.; Butts, C. P.; Bifulco, G. Quantitative NMR-derived interproton distances combined with quantum mechanical calculations of ^{13}C chemical shifts in the stereochemical determination of conicasterol F, a nuclear receptor ligand from *Theonella swinhoei*. *J. Org. Chem.* **2012**, *77*, 1489−1496.
(15) Sepe, V.; Ummarino, R.; D'Auria, M. V.; Chini, M. G.; Bifulco, G.; Renga, B.; D'Amore, C.; Debitus, C.; Fiorucci, S.; Zampella, A. Conicasterol E, a small heterodimer partner sparing farnesoid X receptor modulator endowed with a pregnane X receptor agonistic activity, from the marine sponge *Theonella swinhoei*. *J. Med. Chem.* **2012**, *55*, 84−93.
(16) Rahm, F.; Hayes, P. Y.; Kitching, W. Metabolites from marine sponges of the genus *Plakortis*. *Heterocycles* **2004**, *64*, 523−575.
(17) Zampella, A.; Giannini, C.; Debitus, C.; D'Auria, M. V. Amphiasterins: a new family of cytotoxic metabolites from the marine sponge *Plakortis quasiamphiaster*. *Tetrahedron* **2001**, *57*, 257−263.
(18) Campagnuolo, C.; Fattorusso, E; Romano, A.; Taglialatela-Scafati, O.; Basilico, N.; Parapini, S.; Taramelli, D. Antimalarial polyketide cycloperoxides from the marine sponge Plakortis simplex. *Eur. J. Org. Chem.* **2005**, 5077−5083.
(19) Fattorusso, E.; Parapini, S.; Compagnuolo, C.; Basilico, N.; Taglialatela-Scafati, O.; Taramelli, D. Activity against *Plasmodium falciparum* of cycloperoxide compounds obtained from the sponge *Plakortis simplex*. *J. Antimicrob. Chemother.* **2002**, *50*, 883−888.
(20) Kossuga, M. H.; Nascimento, A. M.; Reim∼ao, J. Q.; Tempone, A. G.; Taniwaki, N. N.; Veloso, K.; Ferreira, A. G.; Cavalcanti, B. C.; Pessoa, C.; Moraes, M. O.; Mayer, A. M. S.; Hajdu, E.; Berlinck, R. G. S. Antiparasitic, antineuroinflammatory, and cytotoxic polyketides from the marine sponge *Plakortis angulospiculatus* collected in Brazil. *J. Nat. Prod.* **2008**, *71*, 334−339.
(21) Fattorusso, E; Taglialatela-Scafati, O. Marine antimalarials. *Mar. Drugs* **2009**, *7*, 130−152.
(22) Feng, Y.; Davis, R. A.; Sykes, M.; Avery, V. M.; Camp, D.; Quinn, R. J. Antitrypanosomal cyclic polyketide peroxides from the Australian marine sponge *Plakortis* sp. *J. Nat. Prod.* **2010**, *73*, 716−719.
(23) Fattorusso, C.; Persico, M.; Calcinai, B.; Cerrano, C.; Parapini, S.; Taramelli, D.; Novellino, E.; Romano, A.; Scala, F.; Fattorusso, E; Taglialatela-Scafati, O. Manadoperoxides A−D from the Indonesian sponge *Plakortis cfr. simplex*. Further insights on the structure−activity relationships of simple 1,2-dioxane antimalarials. *J. Nat. Prod.* **2010**, *73*, 1138−1145.
(24) Mohammed, R.; Peng, J.; Kelly, M.; Yousaf, M.; Winn, E.; Odde, S.; Bie, Z.; Xie, A.; Doerksen, R. J.; Hamann, M. T. Polyketide-peroxides from a species of Jamaican *Plakortis* (Porifera: Demospongiae). *Aust. J. Chem.* **2010**, *63*, 877−885.
(25) Yong, K. W.; De Voss, J. J.; Hooper, J. N.; Garson, M. J. Configurational assignment of cyclic peroxy metabolites provides an insight into their biosynthesis: isolation of plakortolides, seco-plakortolides, and plakortones from the Australian marine sponge *Plakinastrella clathrata*. *J. Nat. Prod.* **2011**, *74*, 194−207.
(26) Ueoka, R.; Nakao, Y.; Kawatsu, S.; Yaegashi, J.; Matsumoto, Y.; Matsunaga, S.; Furihata, K.; van Soest, R. W. M; Fusetani, N. Gracilioethers A-C, antimalarial metabolites from the marine sponge *Agelas gracilis*. *J. Org. Chem.* **2009**, *74*, 4203−4207.
(27) Kupchan, S. M.; Britton, R. W.; Ziegler, M. F.; Sigel, C. W. Bruceantin, a new potent antileukemic simaroubolide from *Brucea antidysenterica*. *J. Org. Chem.* **1973**, *38*, 178−179.
(28) Stierle, D. B.; Faulkner, D. J. Metabolites of three marine sponges of the genus *Plakortis*. *J. Org. Chem.* **1980**, *45*, 3396−3401.
(29) Compagnone, R. S.; Piña, I. C.; Rangel, H. R.; Dagger, F.; Suárez, A. I.; Reddy, M. V. R.; Faulkner, D. J. Antileishmanial cyclic peroxides from the Palauan sponge *Plakortis* aff. *angulospiculatus*. *Tetrahedron* **1998**, *54*, 3057−3068.
(30) Schmidt, E. W.; Faulkner, D. J. Absolute configuration of methyl (2Z,6R,8R,9E)-3,6-epoxy-4,6,8-triethyl-2,4,9-dodecatrienoate from the sponge *Plakortis halichondrioides*. *Tetrahedron Lett.* **1996**, *37*, 6681−6684.
(31) Akiyama, M.; Isoda, Y.; Nishimoto, M.; Kobayashi, A.; Togawa, D.; Hirao, N.; Kuboki, A.; Ohira, S. Stereocontrolled synthesis of (±)-methyl 3,6-epoxy-4,6,8-triethyl-2,4,9-dodecatrienoate, a major metabolite of Caribbean sponge, *Plakortis halichondrioides*, using reactions of alkylidenecarbenes in one pot. *Tetrahedron Lett.* **2005**, *46*, 7483−7485.
(32) Akiyama, M.; Isoda, Y.; Nishimoto, M.; Narazaki, M.; Oka, H.; Kuboki, A.; Ohira, S. Total synthesis and absolute stereochemistry of plakortone E. *Tetrahedron Lett.* **2006**, *47*, 2287−2290.
(33) Selected ^1H NMR for aldehyde **14**: δ 9.53 (s), 6.73 (s), 1.12 (t, J = 7.2 Hz), 0.94 (t, J = 7.1 Hz), 0.85 (t, J = 7.1 Hz); $[\alpha]_D^{25}$ −3.4 (*c* 0.08, $CHCl_3$) aldehyde **14** from **1**; $[\alpha]_D^{25}$ −4.9 (*c* 0.15, $CHCl_3$) aldehyde **14** from **3**.
(34) **2**: $[\alpha]_D^{25}$ −69.2 (*c* 0.20, $CHCl_3$) authentic sample; $[\alpha]_D^{25}$ −68.4 (*c* 0.16, $CHCl_3$) sample from **1**.
(35) Plakilactone A (**7**): $[\alpha]_D^{25}$ −9.5 (*c* 0.12, MeOH) authentic sample; $[\alpha]_D^{25}$ −10.5 (*c* 0.15, MeOH) sample from **2**.
(36) Ohtani, I.; Kusumi, T.; Kashman, Y.; Kakisawa, H. High-field FT NMR application of Mosher's method. The absolute configurations of marine terpenoids. *J. Am. Chem. Soc.* **1991**, *113*, 4092−4096.
(37) Shiraky, T.; Kamiya, N.; Shiki, S.; Kodama, T. S.; Kakizuka, A.; Jingami, H. α,β-Unsaturated ketone is a core moiety of natural ligands for covalent binding to peroxisome proliferator-activated receptor γ. *J. Biol. Chem.* **2005**, *280*, 14145−14153.
(38) Itoh, T.; Fairall, L.; Amin, K.; Inaba, Y.; Szanto, A.; Balint, B. L.; Nagy, L.; Yamamoto, K.; Schwabe, J. W. R. Structural basis for the activation of PPARγ by oxidized fatty acids. *Nat. Struct. Mol. Biol.* **2008**, *15*, 924−931.
(39) Waku, T.; Shiraki, T.; Oyama, T.; Fujimoto, Y.; Maebara, K.; Kamiya, N.; Jingami, H.; Morikawa, K. Structural insight into PPARγ activation through covalent modification with endogenous fatty acids. *J. Mol. Biol.* **2009**, *385*, 188−199.
(40) Monti, M. C.; Margarucci, L.; Tosco, A.; Riccio, R.; Casapullo, A. New insights on the interaction mechanism between tau protein and oleocanthal, an extra-virgin olive-oil bioactive component. *Food Funct.* **2011**, *2*, 423−428.
(41) Monti, M. C.; Chini, M. G.; Margarucci, L.; Riccio, R.; Bifulco, G.; Casapullo, A. The binding mode of cladocoran A to the human group IIA phospholiase A2. *ChemBioChem* **2011**, *12*, 2686−2691.
(42) Monti, M. C.; Casapullo, A.; Cavasotto, C. N.; Tosco, A.; Dal Piaz, F.; Ziemys, A.; Margarucci, L.; Riccio, R. The binding mode of petrosaspongiolide M to the human group IIA phospholipase A2: exploring the role of covalent and non-covalent interactions in the inhibition process. *Chem.—Eur. J.* **2009**, *15*, 1155−1163.
(43) Davies, G. F.; McFie, P. J.; Khandelwal, R. L.; Roesler, W. J. Unique ability of troglitazone to up-regulate peroxisome proliferator-activated receptor-gamma expression in hepatocytes. *J. Pharmacol. Exp. Ther.* **2002**, *300*, 72−77.

(44) Ciudin, A.; Hernandez, C.; Simo, R. Update on cardiovascular safety of PPARgamma agonists and relevance to medicinal chemistry and clinical pharmacology. *Curr. Top. Med. Chem.* **2012**, *12*, 585−604.
(45) Trott, O.; Olson, A. J. AutoDock Vina: improving the speed and accuracy of docking with a new scoring function, efficient optimization, and multithreading. *J. Comput. Chem.* **2010**, *31*, 455−461.
(46) Hughes, T. S.; Chalmers, M. J.; Novick, S.; Kuruvilla, D. S.; Chang, M. R.; Kamenecka, T. M.; Rance, M.; Johnson, B. A.; Burris, T. P.; Griffin, P. R.; Kojetin, D. J. Ligand and receptor dynamics contribute to the mechanism of graded PPARγ agonism. *Structure* **2012**, *20*, 139−150.
(47) Morris, G. M.; Huey, R.; Lindstrom, W.; Sanner, M. F.; Belew, R. K.; Goodsell, D. S.; Olson, A. J. AutoDock4 and AutoDockTools4: Automated docking with selective receptor flexibility. *J. Comput. Chem.* **2009**, *30*, 2785−2791.
(48) Raskin, P.; Rendell, M.; Riddle, M. C.; Dole, J. F.; Freed, M. I.; Rosenstock, J. A randomized trial of rosiglitazone therapy in patients with inadequately controlled insulin-treated type 2 diabetes. *Diabetes Care* **2001**, *24*, 1226−1232.
(49) Mattoo, V.; Eckland, D.; Widel, M.; Duran, S.; Fajardo, C.; Strand, J.; Knight, D.; Grossman, L.; Oakley, D.; Tan, M. Metabolic effects of pioglitazone in combination with insulin in patients with type 2 diabetes mellitus whose disease is not adequately controlled with insulin therapy: results of a six-month, randomized, double-blind, prospective, multicenter, parallel-group study. *Clin. Ther.* **2005**, *27*, 554−567.
(50) Nissen, S. E.; Nicholls, S. J.; Wolski, K.; Nesto, R.; Kupfer, S.; Perez, A.; Jure, H.; De Larochelliere, R.; Staniloae, C. S.; Mavromatis, K.; Saw, J.; Hu, B.; Lincoff, A. M.; Tuzcu, E. M. Comparison of pioglitazone *vs* glimepiride on progression of coronary atherosclerosis in patients with type 2 diabetes: the PERISCOPE randomized controlled trial. *JAMA* **2008**, *299*, 1561−1573.
(51) Aronoff, S.; Rosenblatt, S.; Braithwaite, S.; Egan, J. W.; Mathisen, A. L.; Schneider, R. L. Pioglitazone hydrochloride monotherapy improves glycemic control in the treatment of patients with type 2 diabetes: a 6-month randomized placebo-controlled dose-response study. The pioglitazone 001 study group. *Diabetes Care* **2000**, *23*, 1605−1611.
(52) Diamond, G. A.; Bax, L.; Kaul, S. Uncertain effects of rosiglitazone on the risk for myocardial infarction and cardiovascular death. *Ann. Intern. Med.* **2007**, *147*, 578−581.
(53) Singh, S.; Loke, Y. K.; Furberg, C. D. Long-term risk of cardiovascular events with rosiglitazone: a meta-analysis. *JAMA* **2007**, *298*, 1189−1195.
(54) Fiorucci, S; Zampella, A; Distrutti, E. Development of FXR, PXR and CAR agonists and antagonists for treatment of liver disorders. *Curr. Top. Med. Chem.* **2012**, *6*, 605−624.
(55) Renga, B.; Mencarelli, A.; D'Amore, C.; Cipriani, S.; Baldelli, F.; Zampella, A.; Distrutti, E.; Fiorucci, S. Glucocorticoid receptor mediates the gluconeogenic activity of the farnesoid X receptor in fasting condition. *FASEB J.* **2012**, *26*, 3021−3031.
(56) Rizzo, G.; Fiorucci, S. PPARs and other nuclear receptors in inflammation. *Curr. Opin. Pharmacol.* **2006**, *6*, 421−427.
(57) Fiorucci, S.; Rizzo, G.; Antonelli, E.; Renga, B.; Mencarelli, A.; Riccardi, L.; Morelli, A.; Pruzanski, M.; Pellicciari, R. Cross-talk between farnesoid-X-receptor (FXR) and peroxisome proliferator-activated receptor gamma contributes to the antifibrotic activity of FXR ligands in rodent models of liver cirrhosis. *J. Pharmacol. Exp. Ther.* **2005**, *315*, 58−68.
(58) Elbrecht, A.; Chen, Y.; Adams, A.; Berger, J.; Griffin, P.; Klatt, T.; Zhang, B.; Menke, J.; Zhou, G.; Smith, R. G.; Moller, D. E. L-764406 is a partial agonist of human peroxisome proliferator-activated receptor gamma. The role of Cys313 in ligand binding. *J. Biol. Chem.* **1999**, *274*, 7913−7922.
(59) Lee, G.; Elwood, F.; McNally, J.; Weiszmann, J.; Lindstrom, M.; Amaral, K.; Nakamura, M.; Miao, S.; Cao, P.; Learned, R. M.; Chen, J. L.; Li, Y. T0070907, a selective ligand for peroxisome proliferator-activated receptor gamma, functions as an antagonist of biochemical and cellular activities. *J. Biol. Chem.* **2002**, *277*, 19649−19657.
(60) Pirat, C.; Farce, A.; Lebègue, N.; Renault, N.; Furman, C.; Millet, R.; Yous, S.; Speca, S.; Berthelot, P.; Desreumaux, P.; Chavatte, P. Targeting peroxisome proliferator-activated receptors (PPARs): development of modulators. *J. Med. Chem.* **2012**, *55*, 4027−4061.
(61) Sanner, M. F. Python: a programming language for software integration and development. *J. Mol. Graphics Modell.* **1999**, *17*, 57−61.